MICROBIOME

Diet-derived metabolites and mucus link the gut microbiome to fever after cytotoxic cancer treatment

Zaker I. Schwabkey[1]†‡, Diana H. Wiesnoski[1] †, Chia-Chi Chang[1]†, Wen-Bin Tsai[1], Dung Pham[1], Saira S. Ahmed[1], Tomo Hayase[1], Miriam R. Ortega Turrubiates[1], Rawan K. El-Himri[1], Christopher A. Sanchez[1], Eiko Hayase[1], Annette C. Frenk Oquendo[1], Takahiko Miyama[1], Taylor M. Halsey[1], Brooke E. Heckel[1], Alexandria N. Brown[1], Yimei Jin[1], Mathilde Raybaud[1], Rishika Prasad[1], Ivonne Flores[1], Lauren McDaniel[1], Valerie Chapa[1], Philip L. Lorenzi[2], Marc O. Warmoes[2], Lin Tan[2], Alton G. Swennes[3]§, Stephanie Fowler[3], Margaret Conner[3], Kevin McHugh[4,5], Tyler Graf[5], Vanessa B. Jensen[6], Christine B. Peterson[7], Kim-Anh Do[7], Liangliang Zhang[7], Yushu Shi[7], Yinghong Wang[8], Jessica R. Galloway-Pena[9], Pablo C. Okhuysen[10], Carrie R. Daniel-MacDougall[11], Yusuke Shono[12], Marina Burgos da Silva[12], Jonathan U. Peled[12,13,14], Marcel R.M. van den Brink[12,13,14], Nadim Ajami[1], Jennifer A. Wargo[1,15], Pavan Reddy[16], Raphael H. Valdivia[17], Lauren Davey[17], Gabriela Rondon[18], Samer A. Srour[18], Rohtesh S. Mehta[18], Amin M. Alousi[18], Elizabeth J. Shpall[18], Richard E. Champlin[18], Samuel A. Shelburne[1,10], Jeffrey J. Molldrem[18,19], Mohamed A. Jamal[1]†, Jennifer L. Karmouch[1]†, Robert R. Jenq[1,4,18]*

Not all patients with cancer and severe neutropenia develop fever, and the fecal microbiome may play a role. In a single-center study of patients undergoing hematopoietic cell transplant ($n = 119$), the fecal microbiome was characterized at onset of severe neutropenia. A total of 63 patients (53%) developed a subsequent fever, and their fecal microbiome displayed increased relative abundances of *Akkermansia muciniphila*, a species of mucin-degrading bacteria ($P = 0.006$, corrected for multiple comparisons). Two therapies that induce neutropenia, irradiation and melphalan, similarly expanded *A. muciniphila* and additionally thinned the colonic mucus layer in mice. Caloric restriction of unirradiated mice also expanded *A. muciniphila* and thinned the colonic mucus layer. Antibiotic treatment to eradicate *A. muciniphila* before caloric restriction preserved colonic mucus, whereas *A. muciniphila* reintroduction restored mucus thinning. Caloric restriction of unirradiated mice raised colonic luminal pH and reduced acetate, propionate, and butyrate. Culturing *A. muciniphila* in vitro with propionate reduced utilization of mucin as well as of fucose. Treating irradiated mice with an antibiotic targeting *A. muciniphila* or propionate preserved the mucus layer, suppressed translocation of flagellin, reduced inflammatory cytokines in the colon, and improved thermoregulation. These results suggest that diet, metabolites, and colonic mucus link the microbiome to neutropenic fever and may guide future microbiome-based preventive strategies.

INTRODUCTION

One of the most common and potentially serious complications of cancer therapy is neutropenia and subsequent infectious complications, with an estimated mortality of nearly 10% (*1*) as well as 100,000 hospitalizations and more than $2.7 billion in hospitalization costs annually in the United States (*2*). At particularly high risk are patients undergoing chemotherapy for hematological malignancies including acute leukemias and high-grade lymphomas, or receiving hematopoietic cell transplantation (HCT) after myeloablative conditioning (*3*).

The degree and duration of neutropenia has long been identified as a critical clinical parameter predicting infection (*4*). More recently, the role of the intestinal microbiome in neutropenia-related infections has been increasingly appreciated, with most documented bacterial infections arising from the gastrointestinal tract (*5*, *6*). Most patients, however, will not have an infectious etiology identified, and it is not well understood why only some 50% of patients with profound neutropenia become febrile. Observational studies on patients with acute myeloid leukemia (AML) have described alteration to the gut microbiome, known as dysbiosis, detected at the first episode of febrile neutropenia (*7*). In addition, metabolic profiling has suggested a loss of microbiota-derived protective metabolites during episodes of febrile neutropenia (*8*). Similar studies in the pediatric patients undergoing HCT have linked the longer duration of febrile neutropenia to a higher degree of gut dysbiosis (*9*). However, pathophysiology of the potential role played by typically nonpathogenic intestinal commensal bacteria has not been extensively studied. Here, we sought to gain insight into the contribution of the gut microbiome to the pathophysiology of neutropenic fever using a combination of human samples and experimental mouse models.

RESULTS

The composition of intestinal bacteria at onset of neutropenia is associated with subsequent development of fever

We began with an examination for a potential relationship between the composition of intestinal bacteria and fever in patients who developed neutropenia in the setting of HCT. We examined a cohort

of 119 patients at the University of Texas MD Anderson Cancer Center who all developed neutropenia after HCT conditioning. Of these, 56 (47%) remained afebrile over the next 4 days, whereas 63 (53%) developed a fever, of which 7 were found to have a bloodstream infection, including 5 with Enterobacteriaceae and 2 with oral streptococci. The initial microbiome analyses described below include these seven patients with bloodstream infections with those who developed fever. Before stool collection, patients were treated with prophylactic levofloxacin given daily per our institutional standard. Additional patient characteristics are provided in Table 1. Receiving either an autologous HCT or an HCT after a preparative regimen based on both busulfan and melphalan was associated with increased fever (Table 1), likely reflecting increased conditioning intensity.

We evaluated stool samples collected at the onset of neutropenia, which preceded potential development of fever in all eligible patients. In these samples, we compared the microbiome between those patients who did or did not develop fever over the next 4 days, finding a significant difference in β-diversity [$P = 0.02$, permutational multivariate analysis of variance (MANOVA); Fig. 1A]. Patients who later developed fever had increased relative abundance of bacteria from the genus *Akkermansia* ($P = 0.006$, adjusted for multiple comparisons), as well as bacteria from the genus *Bacteroides* ($P = 0.01$), whereas bacteria from the class Bacilli and from the order Erysipelotrichales were increased in patients who were afebrile (Fig. 1, B to D). Applying a relative abundance threshold of 0.1% to classify patients as having high or low abundances of *Akkermansia* showed a significant association between high *Akkermansia* with subsequent fever (Fisher's test, $P = 0.02$), with 32% of afebrile patients having high *Akkermansia* in comparison to 54% of febrile patients. Similarly, an abundance threshold of 5% to classify patients as having high or low abundances of *Bacteroides* also showed a significant association between high *Bacteroides* with subsequent fever (Fisher's test, $P = 0.0009$), with 37% of afebrile patients having high *Bacteroides* in comparison to 68% of febrile patients. Bacterial taxa associated with bloodstream infections, including Enterobacteriales, *Streptococcus*, and *Enterococcus* (*10*), were not associated with fever.

The recently identified genus *Akkermansia* currently includes only one species present in the intestinal tract of mammals, *Akkermansia muciniphila*, whereas *Bacteroides* is quite diverse. *A. muciniphila* and several members of *Bacteroides* are known to have mucin-degrading capabilities (*11*), and so we asked whether intestinal bacteria from patients with febrile neutropenia had an increased ability to degrade mucin glycans. We adapted an approach where certain carbohydrates including mucin glycans can be quantified from liquid samples using periodic acid–Schiff's reagent (fig. S1, A and B) (*12*). We found that this method could quantify the concentrations of glycans derived from commercially available porcine gastric mucin in medium. After a 48-hour culture, we quantified a reduction in glycan concentration in medium inoculated with isolates of *A. muciniphila* [American Type Culture Collection (ATCC) BAA-835] or *Bacteroides thetaiotaomicron* (ATCC 29148), but glycan concentrations were not altered by an isolate of *Escherichia coli* that does not degrade mucin despite abundant growth (ATCC 700926; fig. S1C). We applied this assay to aliquots of patient fecal samples from Fig. 1 and found that samples from patients with higher combined relative abundances of *Akkermansia* and *Bacteroides* were more effective at consuming mucin glycans (Fig. 1E).

We asked whether introducing the flora of neutropenic patients who later developed fever to germ-free mice could mediate harm after cytotoxic therapy. We used total body radiotherapy (9-Gy RT) as a model of systemic cytotoxic therapy that induces neutropenia and noninvasively monitored ocular surface temperatures to quantify morbidity (*13*). In contrast to humans, mice develop hypothermia in response to exposure to inflammatory ligands such as lipopolysaccharide (*14*) as well as in models of sepsis (*15*), an observation attributed possibly to differences in body size. We found that, as expected, RT induced hypothermia in specific pathogen–free (SPF) mice, with an about 2°C reduction seen on day 5, a time point chosen because some mice would often become moribund by days 6 and 7 (fig. S2A). We thus used hypothermia as a murine surrogate for studying morbidity after RT. Applying this model to patient avatar mice, we found that avatars of febrile and afebrile patients had similar degrees of hypothermia after RT (fig. S2B). In unirradiated mice, differences in the relative abundances of *Akkermansia* were continued to be observed, demonstrating some compositional stability after introduction of patient fecal samples. However, after RT, afebrile avatar mice no longer showed a reduced relative abundances of *Akkermansia* compared to febrile avatar mice (fig. S2, C and D). Together, these results indicate that there was no impact of the introduced patient microbiome on radiation-induced hypothermia nor microbiome composition after cytotoxic therapy. Rather, RT itself led to compositional

[1]Department of Genomic Medicine, The University of Texas MD Anderson Cancer Center, Houston, TX 77030, USA. [2]Department of Bioinformatics and Computational Biology, The University of Texas MD Anderson Cancer Center, Houston, TX 77030, USA. [3]Department of Molecular Virology and Microbiology, Baylor College of Medicine, Houston, TX 77030, USA. [4]CPRIT Scholar in Cancer Research, Austin, TX 78701, USA. [5]Department of Bioengineering, Rice University, Houston, TX 77251, USA. [6]Department of Veterinary Medicine and Surgery, The University of Texas MD Anderson Cancer Center, Houston, TX 77030, USA. [7]Department of Biostatistics, The University of Texas MD Anderson Cancer Center, Houston, TX 77030, USA. [8]Department of Gastroenterology, Hepatology and Nutrition, The University of Texas MD Anderson Cancer Center, Houston, TX 77030, USA. [9]Department of Veterinary Pathobiology, College of Veterinary Medicine and Biomedical Sciences, Texas A&M University, College Station, TX 77843, USA. [10]Department of Infectious Diseases, The University of Texas MD Anderson Cancer Center, Houston, TX 77030, USA. [11]Department of Epidemiology, The University of Texas MD Anderson Cancer Center, Houston, TX 77030, USA. [12]Department of Immunology, Sloan Kettering Institute, Memorial Sloan Kettering Cancer Center, New York, NY 10065, USA. [13]Weill Cornell Medical College, New York, NY 10021, USA. [14]Adult Bone Marrow Transplantation Service, Department of Medicine, Memorial Sloan Kettering Cancer Center, New York, NY 10065, USA. [15]Department of Surgical Oncology, The University of Texas MD Anderson Cancer Center, Houston, TX 77030, USA. [16]Department of Hematology and Oncology, University of Michigan, Ann Arbor, MI 48109, USA. [17]Department of Molecular Genetics and Microbiology, Duke University School of Medicine, Durham, NC 27710, USA. [18]Department of Stem Cell Transplantation and Cellular Therapy, The University of Texas MD Anderson Cancer Center, Houston, TX 77030, USA. [19]Department of Hematopoietic Biology and Malignancy, The University of Texas MD Anderson Cancer Center, Houston, TX 77030, USA.
*Corresponding author. Email: rrjenq@mdanderson.org
†These authors contributed equally to this work.
‡Present address: H. Lee Moffitt Cancer Center & Research Institute, Tampa, FL 33612, USA.
§Present address: Office of Comparative Medicine, University of Utah, Salt Lake City, UT 84112, USA.

Table 1. Patient characteristics. HCT, hematopoietic cell transplantation; WBC, white blood cell; PCD, plasma cell disorder; MDS, myelodysplastic syndrome; MPN, myeloproliferative neoplasm; MF, myelofibrosis. "Other" includes blastic plasmacytoid dendritic cell neoplasm ($n = 2$), chronic myelogenous leukemia ($n = 1$), germ cell tumor ($n = 1$), systemic sclerosis ($n = 1$), and T cell prolymphocytic leukemia ($n = 1$).

	Combined	No fever	Fever	*P*
Total patients	*n* = 119	*n* = 56	*n* = 63	
Median age (range)	58 years (23–80)	62 years (23–80)	56 years (23–75)	0.12
Gender				
Female	*n* = 49 (41.2%)	*n* = 22 (39.3%)	*n* = 27 (42.9%)	0.69
Male	*n* = 70 (58.8%)	*n* = 34 (60.7%)	*n* = 36 (57.1%)	
Graft type				
Autologous HCT	*n* = 62 (52.1%)	*n* = 22 (39.3%)	*n* = 40 (63.5%)	0.008
Allogeneic HCT	*n* = 57 (47.9%)	*n* = 34 (60.7%)	*n* = 23 (36.5%)	
Neutropenia depth				
WBC 100–500 μl	*n* = 34 (28.6%)	*n* = 15 (26.8%)	*n* = 19 (30.2%)	0.84
WBC <100/μl	*n* = 85 (71.4%)	*n* = 41 (73.2%)	*n* = 44 (60.8%)	
Disease				
Multiple myeloma/PCD	*n* = 43 (36.1%)	*n* = 16 (28.6%)	*n* = 27 (42.9%)	0.11
Acute myeloid leukemia	*n* = 23 (19.3%)	*n* = 12 (21.4%)	*n* = 11 (17.5%)	0.58
Non-Hodgkin's lymphoma	*n* = 20 (16.8%)	*n* = 9 (16.1%)	*n* = 11 (17.5%)	0.84
MDS/MPN/MF	*n* = 12 (10.1%)	*n* = 8 (14.3%)	*n* = 4 (6.3%)	0.22
Acute lymphocytic leukemia	*n* = 11 (9.2%)	*n* = 7 (12.5%)	*n* = 4 (6.3%)	0.34
Hodgkin's lymphoma	*n* = 4 (3.4%)	*n* = 0 (0%)	*n* = 4 (6.3%)	0.12
Other	*n* = 6 (5%)	*n* = 4 (7.1%)	*n* = 2 (3.2%)	0.42
Conditioning regimen				
Busulfan-based	*n* = 33 (27.7%)	*n* = 18 (32.1%)	*n* = 15 (23.8%)	0.41
Melphalan-based	*n* = 64 (53.8%)	*n* = 32 (57.1%)	*n* = 32 (50.8%)	0.58
Busulfan- and melphalan-based	*n* = 17 (14.3%)	*n* = 2 (3.6%)	*n* = 15 (23.8%)	0.0015
Other	*n* = 5 (4.2%)	*n* = 4 (7.1%)	*n* = 1 (1.6%)	0.19
Conditioning intensity				
Myeloablative	*n* = 101 (84.9%)	*n* = 44 (78.6%)	*n* = 57 (90.5%)	0.08
Nonmyeloablative	*n* = 12 (21.4%)	*n* = 12 (9.5%)	*n* = 6 (9.5%)	

changes in mice resembling the microbiome profile of febrile patients.

We asked whether, similarly to mice, cytotoxic therapy in patients could induce changes in relative abundances of bacteria of patients undergoing HCT. For most patients from our cohort (32 of 56 without fever and 44 of 63 with fever), baseline stool samples were collected at least 4 days before onset of neutropenia and available for comparison. We found that patients who later developed fever had significantly increased *Akkermansia* and reduced Bacilli at onset of neutropenia compared to baseline, whereas afebrile patients had no significant changes over time in any of the bacteria associated with fever ($P = 0.003$ and $P = 0.037$; Fig. 1F and fig. S2E). In summary, we identified an increase in the relative abundance of bacteria with mucolytic properties in neutropenic patients who later developed fever, and *Akkermansia* in particular was increased in patients who later developed fever.

Radiation or chemotherapy can change the composition of intestinal bacteria in mice, leading to increases in *Akkermansia* and thinning of the dense colonic mucus layer

The fact that our previous analyses had been performed only in patients not receiving broad-spectrum antibiotics suggested that a non-antimicrobial mechanism was mediating the increased relative abundance of mucolytic bacteria. Our patient avatar results also suggested that cytotoxic therapy could modulate the composition of the microbiome into a profile similar to that of patients who develop fever. Thus, we sought to test the hypothesis that transplant conditioning could change the composition of the intestinal microbiome, beginning with total body RT. Normal SPF C57BL/6 mice were exposed to 9-Gy RT, and their stool samples were evaluated 6 days later by 16*S* ribosomal RNA (rRNA) gene sequencing. Similar to what we observed in afebrile avatar mice, the microbiome of SPF mice on day 6 after RT was changed compared to unirradiated mice (Fig. 2A). The profile was reminiscent of that seen in patients undergoing HCT who had febrile neutropenia, showing increases in the relative abundance of *Akkermansia* and, to a lesser degree, *Bacteroides* (Fig. 2, B to D). We did not observe compensatory reductions in Bacilli or Erysipelotrichales, as was observed in patients with febrile neutropenia. Rather, we found reductions in bacteria from the family Muribaculaceae, a recently named group of bacteria that is commonly found in high relative abundance in mice but is usually a minor contributor in the intestinal tract of humans (*16*). We asked whether this change in bacterial composition was accompanied by functional changes and found that bacteria derived from stool samples of irradiated mice more efficiently degraded mucin glycans than bacteria from unirradiated mice in vitro (Fig. 2E). We then asked whether the dense colonic mucus layer, which normally separates bacteria-rich luminal contents from the colonic epithelium, was affected by irradiation in mice. To evaluate this, colonic tissue samples were cut cross-sectionally, and mucus layer thickness was averaged across eight equally spaced circumferential sites (fig. S3). We found that the mucus layer was significantly thinner in irradiated mice compared to normal mice ($P = 0.003$; Fig. 2F).

Myeloablative RT, a foundational pillar that made HCT possible, has been progressively replaced by chemotherapy, particularly alkylating agents (*17*). We thus evaluated treating mice with the alkylating agent melphalan and found that this led to significant changes in the microbiome, marked by an increase in the relative abundance

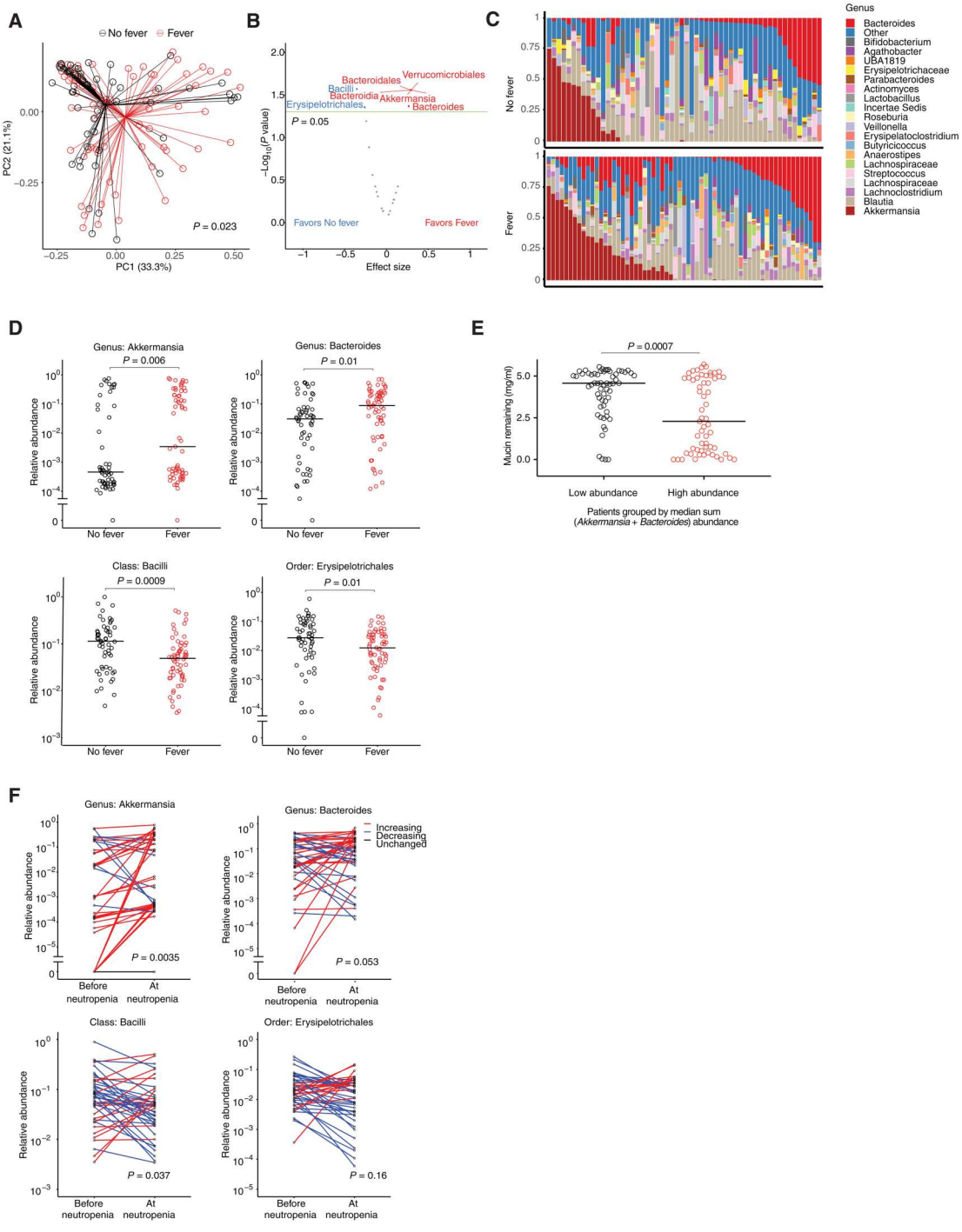

Fig. 1. Mucin-degrading intestinal bacteria are associated with development of fever after onset of post-HCT neutropenia. Intestinal microbiome parameters at neutropenia onset and subsequent fever were evaluated in a cohort of patients undergoing HCT. Stool samples were collected at onset of neutropenia (±2 days), and fever outcome was determined by inpatient monitoring every 4 hours in the subsequent 4 days after collection. (**A**) Principal coordinates of analysis (PCoA) was performed on weighted UniFrac distances based on 16*S* rRNA gene sequencing. Statistical significance was determined by permutational MANOVA testing. (**B**) Volcano plot of bacterial taxa that were differentially abundant in (A). Taxa above the green line have a *P* value less than 0.05; *P* values were adjusted for multiple comparisons using the Benjamini-Hochberg method. (**C**) Relative abundances of bacteria at the genus level in samples from (A) are indicated in stacked bar graphs. (**D**) Relative abundances of bacteria of the indicated taxa are depicted for samples from (A); *P* values were adjusted for multiple comparisons. (**E**) Mucin glycan consumption by frozen aliquots of stool samples in (A) was assayed. Fecal bacteria were cultivated in liquid medium supplemented with porcine gastric mucin as the predominant source of carbon, followed by quantification of remaining mucin glycans after 48 hours. Samples were stratified by median sum relative abundance of *Akkermansia* and *Bacteroides*. Statistical significance was determined by the Mann-Whitney *U* test. (**F**) In the subset of patients who later developed neutropenic fever, relative abundances of bacteria from the indicated taxa in stool samples collected at onset of neutropenia were compared to results of a baseline stool sample collected earlier in the hospitalization, using the Wilcoxon signed-rank test.

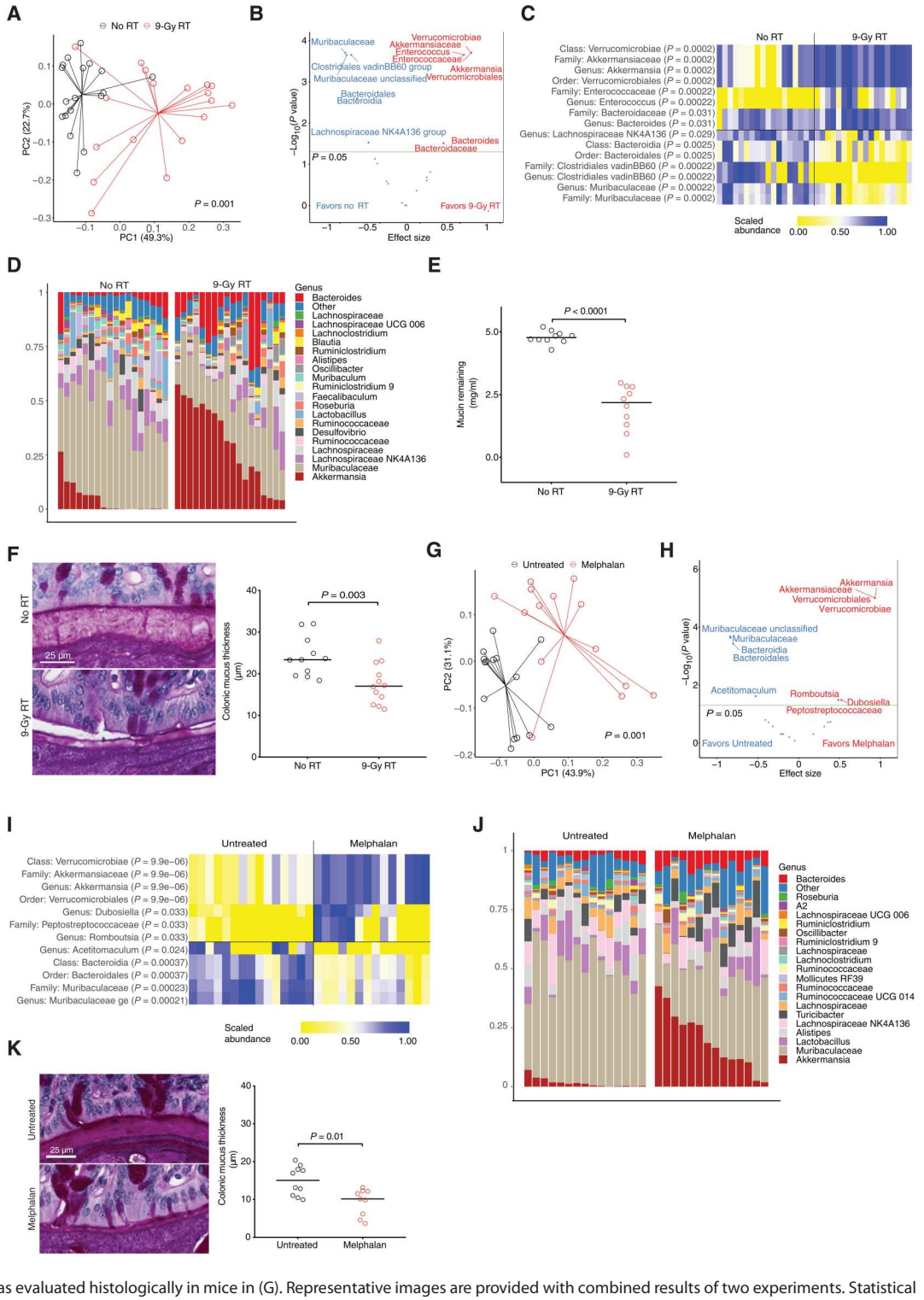

Fig. 2. Systemic cytotoxic therapy increases the relative abundance of mucin-degrading intestinal bacteria in mice. Evaluation of intestinal microbiome parameters was performed in adult C57BL/6 female mice 6 days after total body RT [9-Gy RT; (A) to (E)] or 6 days after melphalan therapy [20 mg/kg; (G to K)]. (**A**) After 9-Gy RT, PCoA was performed on weighted UniFrac distances; combined results of three experiments. Statistical significance was determined by permutational MANOVA testing. (**B**) Volcano plot of bacterial taxa that were differentially abundant in (A); *P* values were adjusted for multiple comparisons using the Benjamini-Hochberg method. (**C**) Heatmap of scaled relative bacterial relative abundances of the indicated taxa is depicted for samples from (A). (**D**) Relative abundances of bacteria at the genus level in samples from (A) are indicated in stacked bar graphs. (**E**) Bacteria from frozen stool samples collected from mice in (A) were evaluated for mucin glycan consumption; combined results of two experiments. Statistical significance was determined by the Mann-Whitney *U* test. (**F**) Thickness of the dense inner colonic mucus layer was evaluated histologically in mice in (A). Representative images are provided with combined results of three experiments. Statistical significance was determined by the Mann-Whitney *U* test. (**G**) After melphalan therapy, PCoA was performed on weighted UniFrac distances; combined results of three experiments. Statistical significance was determined by permutational MANOVA testing. (**H**) Volcano plot of bacterial taxa that were differentially abundant in (G); *P* values were adjusted for multiple comparisons using the Benjamini-Hochberg method. (**I**) Heatmap of scaled relative bacterial relative abundances of the indicated taxa are depicted for samples from (G). (**J**) Relative abundances of bacteria at the genus level in samples from (G) are indicated in stacked bar graphs. (**K**) Thickness of the dense inner colonic mucus layer was evaluated histologically in mice in (G). Representative images are provided with combined results of two experiments. Statistical significance was determined by the Mann-Whitney *U* test.

of *Akkermansia*, similar to that seen after RT ($P = 0.001$; Fig. 2, G to J). An expansion of *Bacteroides* was not statistically significant after correction for multiple comparisons, although a loss of Muribaculaceae, similar to that after RT, was observed. Histological analysis demonstrated that the mucus layer was significantly thinner in melphalan-treated mice, similar to that after RT ($P = 0.01$; Fig. 2K).

We asked why the intestinal microbiome appeared to be affected similarly in response to different cytotoxic therapies. We first evaluated for direct effects of RT on intestinal bacterial composition by irradiating mouse fecal pellets and cultivating bacteria on agar plates. We then swabbed all bacterial colonies that grew and evaluated their taxonomical composition by 16*S* rRNA gene sequencing. We found that exposure to irradiation resulted in no enrichment for *Akkermansia* or *Bacteroides*, although *Akkermansia* relative abundance was low due to its relatively slow growth rate in vitro (fig. S4A). We also introduced bacteria from irradiated fecal pellets orally to mice previously treated with an oral decontaminating antibiotic cocktail. We again found that exposure to irradiation had no discernible effect on the composition of bacterial populations, including no enrichment for *Akkermansia* or *Bacteroides* (fig. S4B).

Caloric restriction in mice is sufficient to produce changes in the composition of the intestinal bacteria similar to those seen after cytotoxic therapy

Diet is known to be a major determinant of intestinal microbiome composition. We asked whether RT could be affecting the microbiome composition indirectly by causing a reduction in intake of food in mice. We individually housed RT-treated mice in metabolic cages to quantify effects on food and water intake. We found that, within 2 days after RT, mice had reduced their oral intake to about 2 g a day or a 50% reduction (Fig. 3A). To evaluate whether caloric restriction (CR) could affect intestinal microbiome composition and the colonic mucus layer, we took healthy, unirradiated mice and limited their access of chow to 2 g per mouse per day for 7 days. We found that CR resulted in marked changes in the microbiome characterized primarily by expansion of *Akkermansia* and, to a lesser extent, an expansion of *Bacteroides* and loss of Bacilli (Fig. 3, B to E). Mucin glycan degradation was more robust after CR (Fig. 3F), and the colonic mucus layer was also significantly thinner ($P < 0.0001$; Fig. 3G). To evaluate whether CR was affecting mucin production, we evaluated goblet cells and specialized epithelial cells that are the primary producers of mucin in the colon. Neither the numbers of goblet cells per crypt nor the combined surface area of goblet cells in a cross section of colonic tissue was affected by CR (fig. S5A). RNA expression of the gene encoding the predominant mucin in the small and large intestine, *Muc2*, was not changed in colonic tissue homogenates from mice after CR (fig. S5B). Together, these results indicated that a reduction in oral nutrition was sufficient to produce a thinner colonic mucus layer, possibly through an increase in mucin degradation, leading to increased consumption of mucin, whereas the production of mucin appeared to be intact.

Manipulating the intestinal bacteria of mice with different antibiotics and bacterial reintroduction indicates that *Akkermansia* is required for thinning of the colonic mucus layer with CR

Akkermansia is nearly universally found in fecal samples of commercially available mice (*18*). Germ-free mice are available but have been reported to have many derangements in mucosal immunity including an underdeveloped colonic mucus layer (*19*). We confirmed this to be the case, with germ-free mice having a poorly developed colonic mucus thickness. We additionally found that mono-associating mice with a murine isolate of *A. muciniphila* (MDA-JAX AM001) derived from the feces of C57BL/6 mice for 2 weeks was not sufficient to restore a normal-appearing colonic mucus layer (fig. S5C). Thus, to allow evaluation of the contribution of *Akkermansia* to mucus thinning during CR, we turned to narrow-spectrum antibiotics (Fig. 3H). Specifically, we evaluated streptomycin, which we found depleted certain Gram-positive bacteria but spared both *Akkermansia* and *Bacteroides*; vancomycin, which depleted both Gram-positive bacteria and *Bacteroides* but spared *Akkermansia*; and azithromycin, which depleted *Akkermansia* as well as some Gram-positive populations but spared *Bacteroides* (Fig. 3I). Each of these antibiotics was administered continously in the drinking water of mice during CR. We found that neither streptomycin nor vancomycin had a significant effect on mucus thickness, whereas azithromycin treatment prevented thinning of the colonic mucus layer ($P = 0.01$; Fig. 3J), indicating that *Akkermansia* could be required for increased mucolysis during CR.

To further assess the contribution of *Akkermansia* to colonic mucus loss during CR, we evaluated antibiotic strategies that could eradicate *Akkermansia* when administered as a course of therapy that is discontinued before starting CR. Although even high-dose administration of azithromycin was not effective at eradicating *Akkermansia* in mice (fig. S5, D and E), we found that pretreatment with a 3-week course of tetracycline was sufficient to eradicate *Akkermansia*, as had been reported previously (*18*), with relative abundances remaining undetectable after completing treatment even after CR (Fig. 4, A and B). Tetracycline pretreatment resulted in no appreciable thinning of colonic mucus after CR (Fig. 4C). Furthermore, reintroducing *Akkermansia* to tetracycline pretreated mice was sufficient to restore mucus thinning after CR (Fig. 4, B and C). Together, these data indicate that the presence of *Akkermansia* is required and sufficient for increased mucolysis during CR.

Production of short-chain fatty acids is affected by CR

To identify potential mechanistic links between diet and microbiome composition, we hypothesized that CR was perturbing normal commensal bacterial metabolism in the intestinal lumen, and began by asking whether metabolic substrates entering the colon were affected by CR. To evalute this, we performed bomb calorimetry on cecal contents of mice and found that restricted mice had fewer calories entering the colon (Fig. 5A). Among the most abundant products of intestinal bacterial metabolism are organic acids, and thus, we quantified pH in the colonic lumen and found that CR resulted in a raised pH of about 7.2 compared to 6.5, indicating overall reduced metabolism (Fig. 5B). To better characterize this rise in pH, we quantified specific bacterial metabolites using ion chromatography–mass spectrometry and found that CR led to reduced concentrations of acetate, propionate, and butyrate and increased succinate (normalized results in Fig. 5C, raw results in fig. S6A). Succinate is a metabolic precursor of propionate (*20*), suggesting that CR could be inhibiting enzymatic conversion of succinate to propionate.

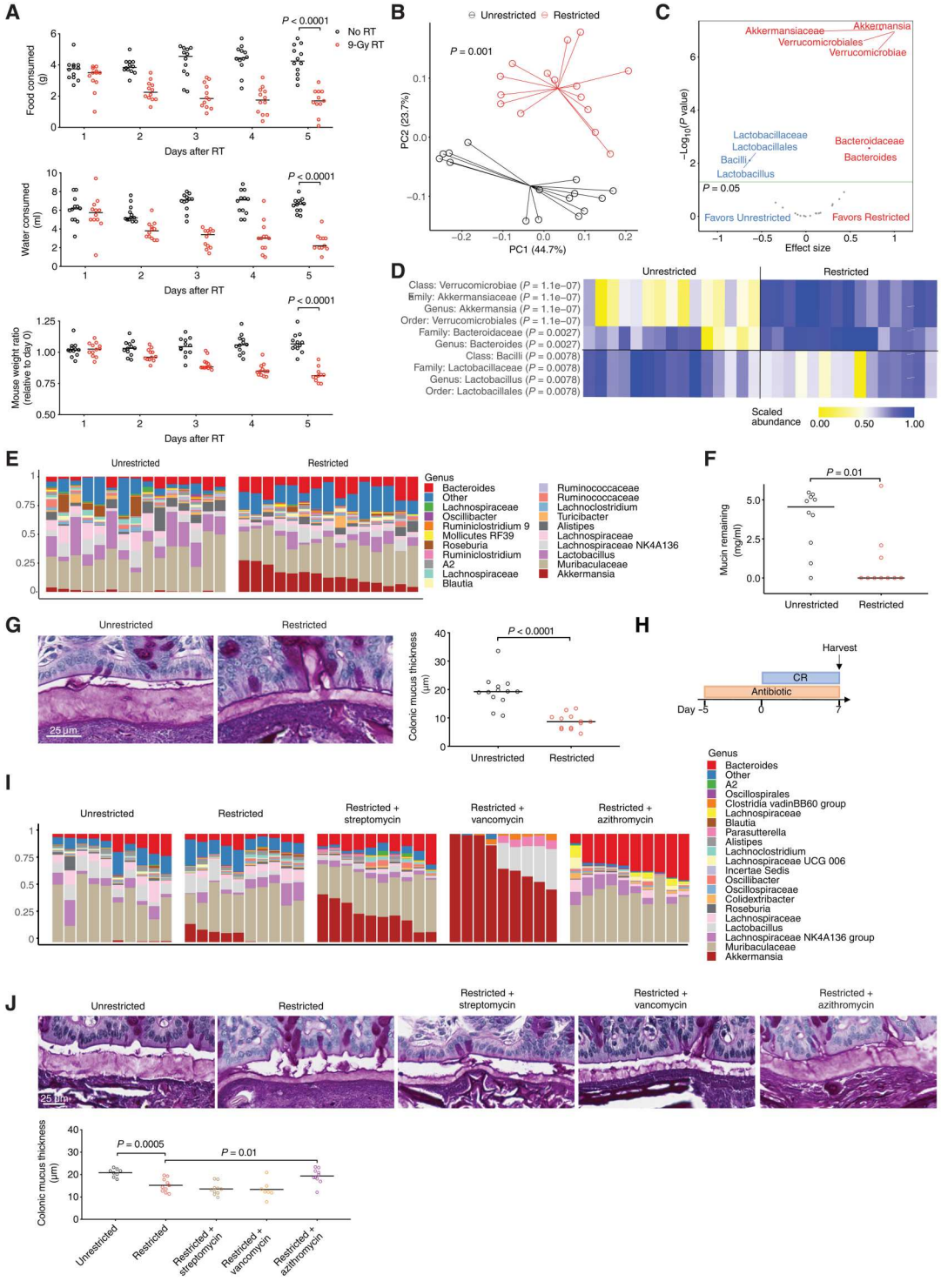

Fig. 3. CR increases the relative abundance of mucin-degrading intestinal bacteria in mice. (**A**) After 9-Gy RT, mice were individually housed in metabolic cages and monitored daily for food consumption, water consumption, and weight. Statistical significance was determined by the Mann-Whitney *U* test. (**B**) Intestinal microbiome parameters were evaluated in normal mice after undergoing CR (2 g per mouse per day) for 1 week. PCoA was performed on weighted UniFrac distances; combined results of three experiments. Statistical significance was determined by permutational MANOVA testing. (**C**) Volcano plot of bacterial taxa that were differentially abundant in (B); *P* values were adjusted for multiple comparisons using the Benjamini-Hochberg method. (**D**) Heatmap of scaled relative bacterial relative abundances of the indicated taxa are depicted for samples from (B). (**E**) Relative abundances of bacteria at the genus level in samples from (A) are indicated in stacked bar graphs. (**F**) Bacteria from frozen stool samples collected from mice in (B) were evaluated for mucin glycan consumption; combined results of two experiments. Statistical significance was determined by the Mann-Whitney *U* test. (**G**) Thickness of the dense inner colonic mucus layer was evaluated histologically in mice in (B). Representative images are provided with combined results of three experiments. Statistical significance was determined by the Mann-Whitney *U* test. (**H**) Experimental schema. Mice underwent CR as in (B), with the addition of narrow-spectrum antibiotics administered in the drinking water starting 5 days before onset of restriction. (**I**) Relative abundances of bacteria at the genus level in samples are indicated in stacked bar graphs; combined results of two experiments. (**J**) Thickness of the dense inner colonic mucus layer was evaluated histologically in mice in (I). Representative images are provided with combined results of two experiments. Statistical significance was determined by the Mann-Whitney *U* test.

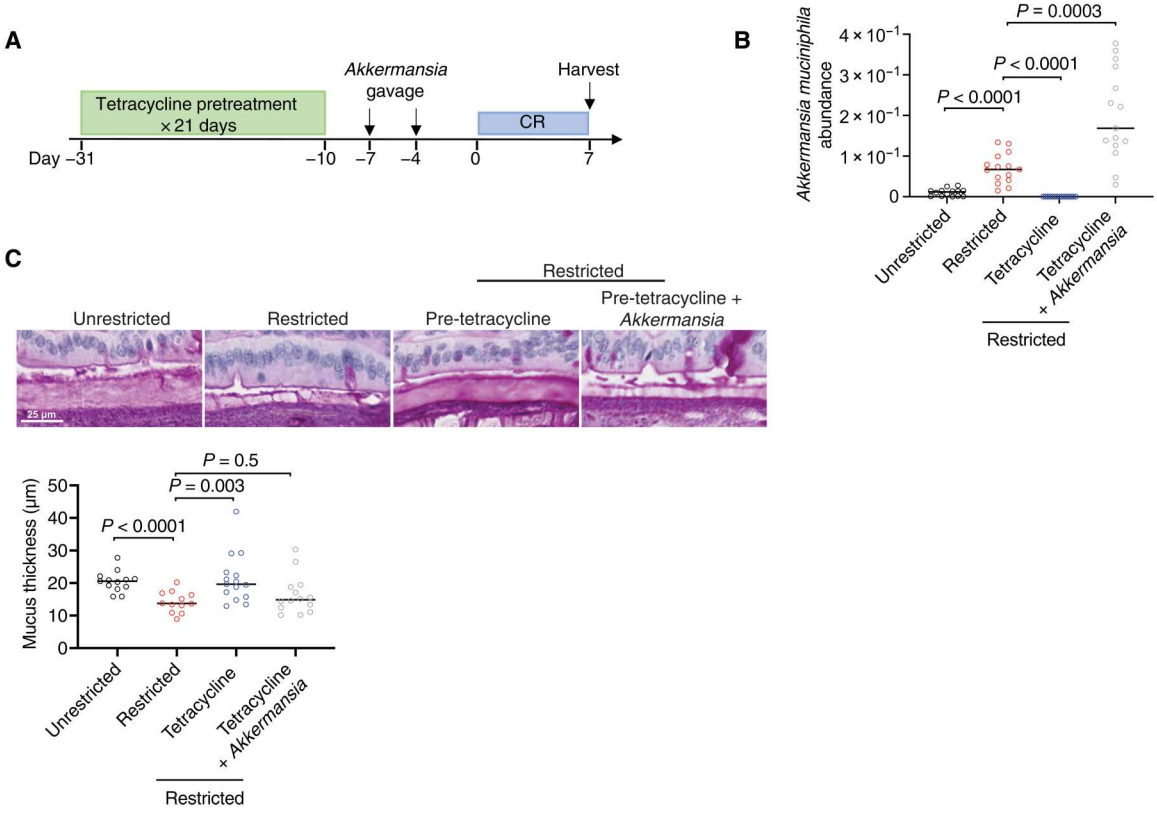

Fig. 4. Akkermansia is required for increased mucus degradation during calorie restriction. (**A**) Experimental schema. Mice were pretreated with tetracycline administered in the drinking water for 21 days to clear the intestines of *A. muciniphila*. A murine isolate of *A. muciniphila* (MDA-JAX AM001) was reintroduced 5 days before the onset of restriction. (**B**) Relative abundances of *Akkermansia* on day 7 after CR were quantified by 16*S* rRNA gene sequencing; combined results of four experiments. Statistical significance was determined by the Mann-Whitney *U* test. (**C**) Thickness of the dense inner colonic mucus layer was evaluated histologically in mice in (B). Statistical significance was determined by the Mann-Whitney *U* test.

Acidity and propionate concentrations inhibit mucin utilization by *Akkermansia* in vitro

We asked whether CR-induced metabolic changes in the colonic lumen affected *A. muciniphila* behavior. To study this, we turned to our in vitro mucin glycan consumption assay. We introduced murine *A. muciniphila* to liquid medium supplemented with porcine gastric mucin and evaluated the effects of varying pH either alone or with physiological concentrations of acetate, propionate, and butyrate. We found that progressively lowering the pH conditions of bacterial medium led to increased inhibition of *A. muciniphila* in terms of both growth and mucin glycan degradation (Fig. 5D). We also found that higher concentration of propionate had inhibitory effects on mucin glycan utilization by *A. muciniphila* (Fig. 5E) and led to growth delays (fig. S6B), whereas acetate and butyrate each had negligible effects on *A. muciniphila* behavior. We also evaluated the effects of acetate, propionate, and butyrate at concentrations beyond physiological concentration on *A. muciniphila* in pH 6.8 conditions. We found that propionate inhibited mucin consumption at a concentration of 10 mM and further increasing the concentration led to increased inhibition of *A. muciniphila* growth, with complete growth inhibition occuring at 40 mM (Fig. 5, F and G). Butyrate was less potent, with 40 mM required to suppress mucin consumption and concentration of 100 mM required to complete growth. Acetate, even at high concentrations, had only slightly suppressive effects on *A. muciniphila* mucin degradation and growth. Together, these results demonstrated that propionate and, to a lesser degree, butyrate, as well as acidity, have suppressive effects on the utilization of mucin by *A. muciniphila*.

We asked whether this finding that propionate can inhibit mucin glycan degradation by *A. muciniphila* was potentially true for other species of bacteria. To evaluate this, we examined mucin utilization in vitro by strains of *Bacteroides* (*21*, *22*), *Parabacteroides* (*23*), *Alistipes* (*24*), *Bifidobacterium* (*25*), and *Ruminococcus* (*26*–*28*). These data demonstrated that propionate can suppress mucin utilization by *Parabacteroides distasonis*, but not that of other mucin degraders tested (fig. S7A).

Acidified propionate administration during CR prevents thinning of colonic mucus

To see whether a combination of acidity and propionate could also suppress *A. muciniphila* in vivo, we supplemented mice during CR with acidified sodium propionate in the drinking water and found that this reduced fecal pH (fig. S7B), mitigated expansion of *Akkermansia* (Fig. 5H), and prevented thinning of the mucus layer (Fig. 5I). Similar treatment with acidified sodium acetate, despite lowering the pH in the colonic lumen, had no such preventative effect (Fig. 4, H and I), whereas drinking water with sodium propionate at neutral pH was sufficient to prevent mucus thinning (fig.

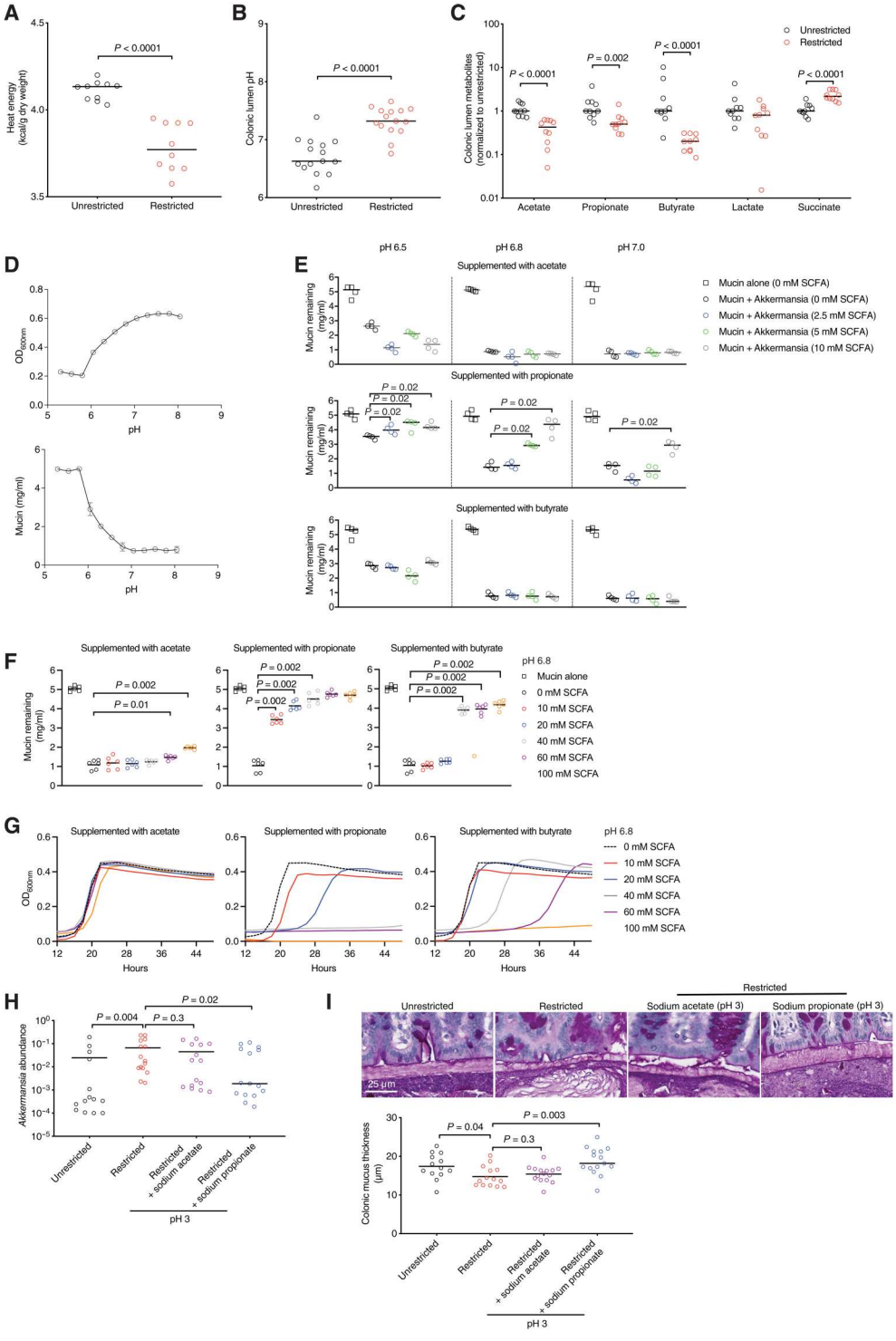

Fig. 5. Bacterial metabolites link CR to mucolytic bacteria. (**A**) In mice that underwent 1 week of CR, cecal luminal contents were assessed for caloric content by bomb calorimetry; combined results of two experiments. (**B**) Colonic luminal contents were assessed for pH in mice after 1 week of CR; combined results of three experiments. (**C**) Metabolites from samples in (B) were quantified using ion chromatography–mass spectrometry; combined results of two experiments. (**D**) Murine *A. muciniphila* (MDA-JAX AM001) was cultivated under anaerobic conditions of varying pH in four replicates, and growth and mucin glycan consumption were quantified after 48 hours of culture; results of one of two experiments with similar results. $P < 0.0001$, growth of *A. muciniphila* at pH 5.0 versus pH 6.75; $P = 0.03$, mucin degradation at pH 5.0 versus pH 6.75. (**E**) Murine *A. muciniphila* (MDA-JAX AM001) was cultivated under varying pH and varying concentrations of sodium acetate, sodium propionate, and sodium butyrate in four replicates, and mucin glycan consumption was quantified after 48 hours of culture; results of one of two experiments with similar results. pH 6.8: $P = 0.03$, 0 mM versus 5 and 10 mM propionate; P = not significant (NS), 0 mM versus 2.5 mM propionate; P = NS, 0 mM versus 2.5, 5, and 10 mM acetate and butyrate. (**F**) Murine *A. muciniphila* (MDA-JAX AM001) was cultivated with varying concentrations of sodium acetate, sodium propionate, and sodium butyrate. Mucin glycan consumption was quantified after 24 hours of culture. Values are shown as averages; results of three experiments. $P = 0.002$, 0 mM versus 10 and 20 mM propionate; P = NS, 0 mM versus 10 and 20 mM acetate and butyrate. (**G**) Murine *A. muciniphila* was cultivated with SCFAs as in (F). Growth was monitored continuously up to 48 hours. Values are shown as averages; results of one of two experiments with similar results. OD_{600nm}, optical density at 600 nm. (**H**) Normal mice received 1 week of CR, as well as supplementation with sodium acetate or sodium propionate in the drinking water, acidified to pH 3. Relative abundances of *Akkermansia* were quantified by 16*S* rRNA gene sequencing; combined results of three experiments. (**I**) Thickness of the dense inner colonic mucus layer was evaluated histologically in mice in (F). Representative images are provided with combined results of three experiments.

S7, C and D). Together, these results indicate that a reduced concentrations of propionate after CR and a higher pH together support increased mucolytic activity.

CR or cultivation in ambient propionate produces transcriptomic changes in *Akkermansia*

To explore how CR can modulate mucin utilization by *A. muciniphila*, we profiled the *A. muciniphila* transcriptome in stool samples collected from mice that were or were not undergoing CR. We determined the circularized genomic sequence of our murine *A. muciniphila* isolate (MDA-JAX AM001) and identified 1757 putative

proteins (fig. S8A), including 1373 that were not annotated as "hypothetical proteins." We then performed RNA sequencing on stool samples from mice and considered reads that aligned to the *A. muciniphila* genome to quantify the relative abundance of individual gene transcripts expressed by *A. muciniphila*. Focusing on the 100 most variable genes not annotated as "hypothetical," we found that 38 genes were significantly modulated by CR in vivo (DESeq2 test with Benjamini-Hochberg adjustment, $P < 0.05$; Fig. 6A).

We note that two adjacent genes (136 and 137) encoding fucose utilization proteins were both significantly up-regulated in calorie-restricted mice ($P = 0.0004$ and $P = 0.008$). One is predicted to be an L-fucose transporter, whereas the other encodes an L-fucose isomerase, which converts fucose to fucolose in the first step of bacterial fucose metabolism (*29*). Mucins are proteins decorated by extensive glycan chains that are predominantly capped by fucose and sialic acid residues at their branching terminals. The ATCC type strain of *A. muciniphila* has previously been reported to be capable of using fucose as a carbohydrate source (*30*). Because we had found that propionate is reduced with CR and that propionate can directly suppress mucin glycan utilization by *A. muciniphila*, we asked whether propionate was sufficient to affect expression of these fucose utilization genes in vitro. We cultivated murine *A. muciniphila* with varying concentrations of propionate and performed RNA sequencing. This approach demonstrated that both genes 136 and 137 negatively correlated with ambient propionate concentrations (Fig. 6B), consistent with our in vivo results. We also globally evaluated the correlation of effect sizes in the in vivo and in vitro settings and found that propionate-related effects observed in vitro only explained changes seen in CR at a proportion of 0.05, although the slope was significantly nonzero ($P < 0.0001$; fig. S8B). Representations of gene expression with respect to the genome are depicted in fig. S8C, and relative gene abundances of all in vivo and in vitro samples are provided in data file S1.

Cultivation in ambient propionate reduces expression of L-fucose isomerase by *Akkermansia*

These results led us to ask whether propionate could affect fucose utilization by *A. muciniphilia*. We first evaluated the growth of *A. muciniphilia* in carbohydrate-poor medium supplemented with fucose and found that our murine isolate exhibited better growth in the presence of fucose (Fig. 6C). We also found that the addition of 10 or 20 mM propionate resulted in dose-dependent delays in growth on fucose, as well as reduced consumption of fucose by *A. muciniphilia*, whereas the same concentrations of acetate or butyrate had no appreciable effects (Fig. 6, D and E).

Next, we focused on quantifying the effects of propionate on expression of L-fucose isomerase. We prepared lysates of *A. muciniphilia* that had been cultivated with mucin in varying concentrations of propionate. These lysates were then incubated with fresh L-fucose, and resulting concentrations of both L-fucose and L-fuculose were quantified. Lysates prepared from *A. muciniphilia* grown in the absence of propionate were able to convert L-fucose to generate L-fuculose. Lysates from *A. muciniphilia* cultivated in the presence of propionate, however, did not efficiently catalyze this reaction, resulting in significantly less L-fuculose and higher concentrations of preserved L-fucose ($P < 0.0001$; Fig. 6F). Together, these results indicate that propionate can suppress the utilization and enzymatic metabolism of L-fucose by *A. muciniphilia*, potentially accounting for its reduced ability to consume mucin.

Administration of azithromycin or acidified propionate prevents colonic mucus thinning, colonic inflammation, and hypothermia in mice after radiation

Last, we asked whether either of the two strategies that we had identified as effective in preventing loss of colonic mucin during CR, azithromycin or propionate, could also mediate a clinical benefit after cytotoxic therapy. To evaluate this, we returned to our RT model and tested the addition of azithromycin or propionate. We found that whereas azithromycin was effective at preventing outgrowth of *Akkermansia* in mice after RT, propionate was not (Fig. 7A). Both approaches, however, led to improved preservation of colonic mucus layer thickness (Fig. 7B). Because a thinned mucus layer quantified from fixed tissue does not necessarily imply a compromised barrier, we also characterized the effects of our interventions on intestinal barrier function after RT. We quantified serum concentration of the bacterial product flagellin, which can serve as a measure of compromised gut barrier integrity (*31*, *32*). We found that RT resulted in a significant increase of serum flagellin that could be blocked by the addition of azithromycin or propionate treatment ($P < 0.0001$; Fig. 7C).

These results suggested that strategies to inhibit mucolytic activity of *A. muciniphila* might be effective at reducing inflammation in irradiated mice. To explore this, we characterized inflammation severity in colonic tissues by quantifying the concentration of a panel of cytokines (Fig. 7D). We found that interleukin-1β (IL-1β), CCL2, CCL7, IL-22, CXCL1, and CXCL10 were all elevated in colonic tissues of mice after RT but were reduced with the addition of azithromycin treatment. Propionate treatment also prevented elevation of each of these cytokines, except for CXCL1, which remained elevated. We did not observe elevations of tumor necrosis factor (TNF) after RT, nor effects of azithromycin or propionate on TNF concentrations.

We asked whether strategies to inhibit mucolytic activity of *A. muciniphila*, which we had originally identified to be associated with development of fever in neutropenic patients, could potentially help to prevent fever. We thus evaluated for an impact on RT-induced hypothermia by monitoring surface ocular temperatures. We found that, after RT, mice developed hypothermia as expected. The temperatures of irradiated mice supplemented with azithromycin or propionate, however, were substantially less depressed at day 6 (Fig. 7E). Ocular temperatures of mice across all experimental groups showed an inverse correlation with serum flagellin concentrations ($r = -0.56$, $P = 0.0009$; Fig. 7F).

Together, results from interventional experiments in mice after RT indicated that azithromycin therapy was effective at eliminating intestinal *Akkermansia*, preserving colonic mucus and epithelial integrity, and preventing colonic inflammation and hypothermia, whereas propionate therapy was less effective but nevertheless prevented colonic mucus thinning, improved epithelial integrity, largely abrogated much of the colonic inflammation that occurred after RT, and substantially prevented hypothermia.

DISCUSSION

We found that bacteria with mucin-degrading capabilities, especially *Akkermansia*, were enriched in neutropenic patients who later developed fever, with 32% of afebrile patients having an *Akkermansia* relative abundance greater than 0.1% in comparison to 54% of febrile patients. Mucus degraders, however, have been previously

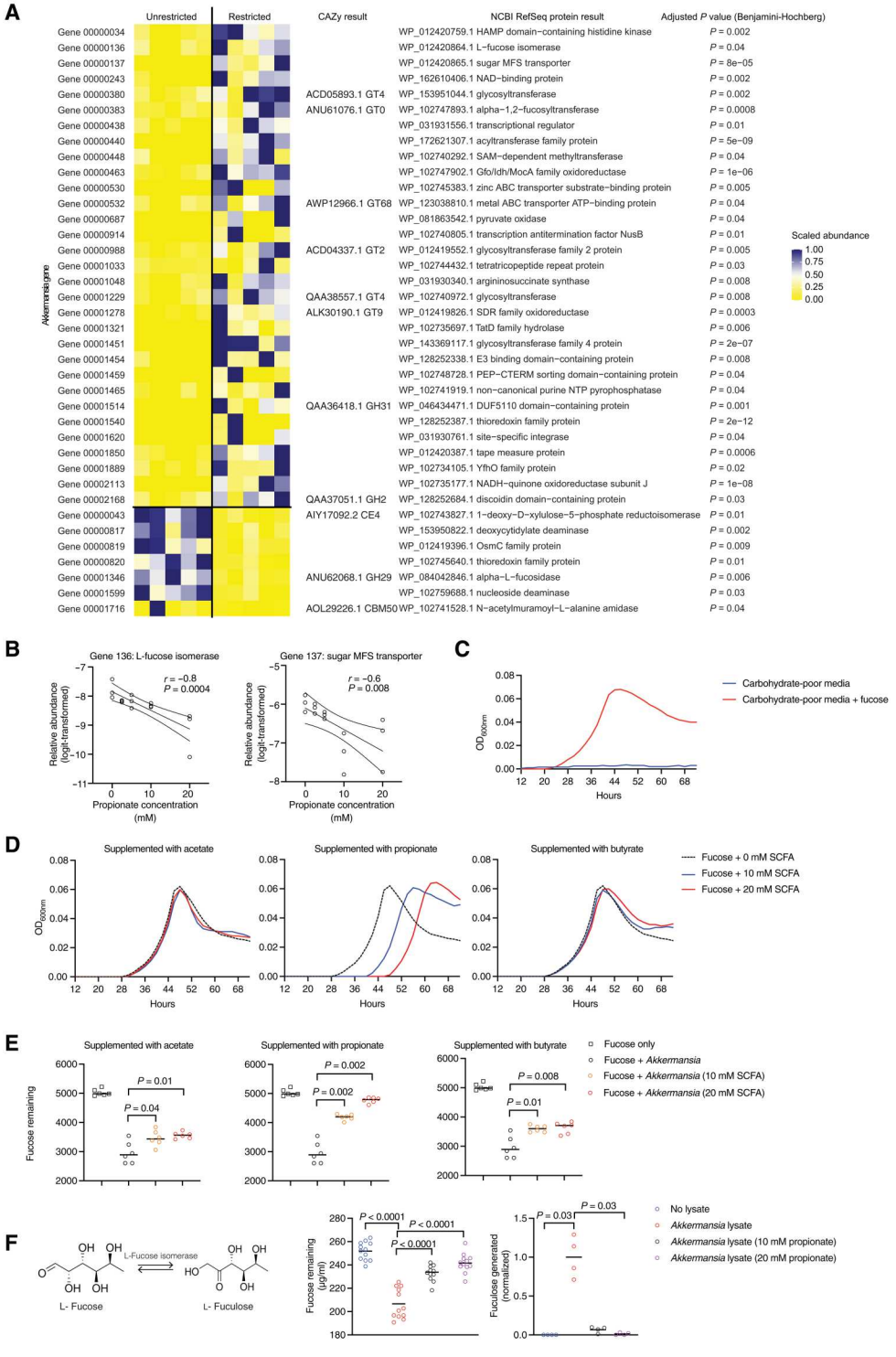

Fig. 6. Propionate suppresses L-fucose utilization by *A. muciniphila*. (**A**) Transcriptomic profiling identifies *A. muciniphila* (MDA-JAX AM001) genes similarly regulated by diet in vivo and propionate in vitro. RNA sequencing was performed on murine *A. muciniphila* cultivated at pH 6.8 with varying concentrations of sodium propionate (as in Fig. 5E) in three replicates (left panel) and on fecal pellets from mice after 1 week of dietary restriction (n = 5; right panel). Sequences aligning with the genome of murine *A. muciniphila* were quantified, and the scaled abundances of the subset of genes similarly regulated by diet and propionate are depicted in the heatmap, along with annotations obtained using both the Carbohydrate-Active enZYmes (CAZy) and National Center for Biotechnology Information (NCBI) Reference Sequencing (RefSeq) Protein databases. (**B**) Relative abundance of fucose isomerase gene (A) and major facilitator superfamily (MFS) transporter gene obtained by RNA sequencing performed on murine *A. muciniphila* cultivated at pH 6.8 with varying concentrations of sodium propionate. (**C**) Murine *A. muciniphila* was cultivated in carbohydrate-poor BYEM10 medium with and without L-fucose supplementation. Growth was monitored continuously up to 72 hours. (**D**) Murine *A. muciniphila* was cultivated with fucose and varying concentrations of sodium acetate, sodium propionate, and sodium butyrate. Growth was monitored continuously up to 72 hours. Values are shown as averages; results from three experiments. (**E**) Murine *A. muciniphila* was cultivated with fucose and varying concentrations of sodium acetate, sodium propionate, and sodium butyrate. Fucose remaining was quantified after 40 hours of culture. Values are shown as averages; results of three experiments. (**F**) Schematic diagram for the conversion of L-fucose to L-fuculose mediated by L-fucose isomerase (left panel). (Middle and right panels) In vitro enzymatic activity of L-fucose isomerase from murine *A. muciniphila* grown in mucin with or without propionate. L-Fucose remaining and L-fuculose generated were quantified after 1-hour incubation. Values are shown as averages; results of three experiments. L-fuculose concentrations were normalized to median L-fuculose concentration of the *Akkermansia* lysate group. Statistical significance for each graphical dataset was determined by the Mann-Whitney U test.

implicated in other disease settings, including inflammatory bowel disease (*28*, *33*), graft-versus-host disease (*34*), and colonic epithelial carcinogenesis (*35*). *A. muciniphila*, identified in 2004 as a specialized intestinal mucin-degrading commensal (*36*), has in particular been associated with increased colitis (*37*) and colonic graft-versus-host disease (*34*) in mouse models. Other mucin degraders include members of the genus *Bacteroides*, which have been associated with murine colitis (*38*) and are particularly well studied because of the availability of methods to manipulate genetically tractable *Bacteroides* isolates (*39*). *Ruminococcus gnavus* is another mucin-degrading species that has been well studied (*40*) and has been clinically associated with inflammatory bowel disease (*41*).

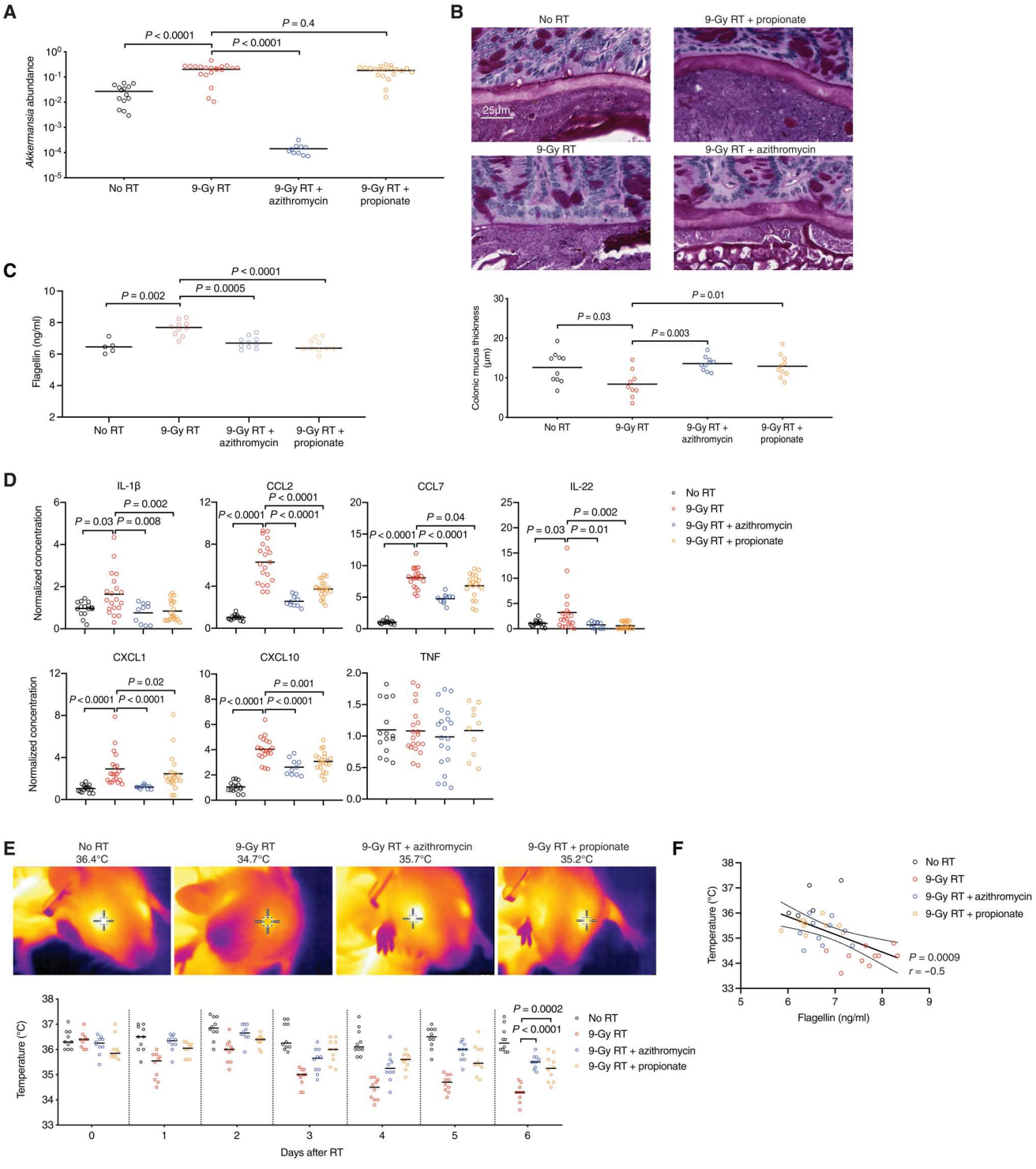

Fig. 7. Strategies targeting mucolytic bacteria in mice receiving RT preserve colonic mucus, reduce hypothermia, and reduce colonic inflammation. In the setting of 9-Gy RT, mice were treated with azithromycin or sodium propionate. (**A**) Relative abundances of *Akkermansia* on day 6 after RT were quantified by 16*S* rRNA gene sequencing; combined results of three experiments. Statistical significance was determined by the Mann-Whitney *U* test. (**B**) Thickness of the dense inner colonic mucus layer was evaluated histologically. Representative images are provided with combined results of two experiments. Statistical significance was determined by the Mann-Whitney *U* test. (**C**) Serum flagellin concentrations were quantified on day 6 after RT. Statistical significance was determined by the Mann-Whitney *U* test. (**D**) On day 6 after RT, mice were harvested, and colonic tissues were processed to quantify concentrations of cytokines; combined results of three experiments. Statistical significance was determined by the Mann-Whitney *U* test. (**E**) Ocular temperatures were monitored daily. Representative images 6 days after RT are provided with combined results of two experiments. Statistical significance was determined by the Mann-Whitney *U* test. (**F**) Quantification of the correlation between flagellin concentrations and ocular temperature on day 6 after RT by Pearson coefficient.

In other clinical settings, *A. muciniphila* is associated with potentially beneficial health effects. Loss of *A. muciniphila* has been observed in individuals with metabolic conditions, including obesity and type 2 diabetes, and supplementation with *A. muciniphila* may mediate a clinical improvement (*42*). Increased *A. muciniphila* has also been associated with enhanced responses to PD1 blockade immunotherapy in patients with lung and urothelial cancers, and superior tumor responses in mice (*43*).

We observed that the relative abundance of *A. muciniphila* increased after cytotoxic chemotherapy in some patients undergoing HCT, reaching as high as 76.6% in some patients who later developed fever. We speculate that this may have been due to poor diet as well as possibly receiving antibiotics before transplant hospitalization, because any patients administered antibiotics during transplant hospitalization were excluded from the study. One limitation of this study is that the abundance of *A. muciniphila* was highly heterogeneous in both afebrile and febrile patients and does not by itself perfectly predict who will or will not develop neutropenic fever. An important question that remains to be answered is whether there are functional strain differences within the microbiome of individual patients, as has been observed in other human cohorts (*44*), and whether particular subclades of *A. muciniphila* are more or less strongly associated with developing neutropenic fever.

RT or melphalan therapy also produced increases in the relative abundance of *A. muciniphila* in mice, and we found that this was likely driven by reductions in oral dietary intake. A link between restrictions in diet and *A. muciniphila* has been observed before, including in subjects after Islamic fasting (*45*) or after as little as 3 days of deliberate underfeeding in the context of a clinical trial (*46*), and has been recently systematically reviewed (*47*). In mice, intermittent 16-hour fasting for 1 month resulted in increased abundance of *A. muciniphila* (*48*), as did 4 days after switching from oral to parenteral nutrition delivered after internal jugular vein catheterization (*49*). Mice consuming a fiber-depleted diet were previously found to have expansions of *A. muciniphila* and mucin-degrading *Bacteroides* as well as compromise of colonic mucus, and this led to increased susceptibility to colitis secondary to *Citrobacter rodentium* (*30*), findings that likely have shared mechanisms with our findings in calorie-restricted mice.

Why diet and *A. muciniphila* are closely linked is not as well understood. We found that propionate concentrations in the intestinal lumen were reduced with CR and that propionate mediated suppressive effects on utilization of mucin glycans by *A. muciniphila*. In addition to *A. muciniphila*, *Staphylococcus aureus* has also been shown to be inhibited by propionate, whereas acetate and butyrate were not effective (*50*). *A. muciniphila* has been reported to produce propionate after metabolism of mucin-derived carbohydrates (*51*, *52*), and thus, the presence of propionate, as a metabolic end product, may serve as a feedback mechanism to suppress excessive utilization of mucin glycans. Inhibition of *A. muciniphila* by propionate was more pronounced at lower pH settings, which could be due to better penetration of propionate through bacterial cell membranes in its protonated state, as has been recently observed for acetate uptake by Enterobacteriaceae (*53*). The mechanism by which propionate suppresses mucin utilization by *A. muciniphila*, however, remains unclear and is a limitation of our study. In addition, whether other colonic lumen metabolites besides short-chain fatty acids (SCFAs) could additionally mediate suppression remains an unanswered question.

In our study, we focused on intestinal bacteria, especially *Akkermansia*, and effects mediated by propionate on *Akkermansia*. It is important to acknowledge, however, that propionate likely has effects on other intestinal commensal bacteria and is also known to have an impact on a variety of host cell types, including epithelial and immune cells. Propionate has been demonstrated to mediate these effects through several signaling pathways and epigenetic mechanisms. For example, in ileal organoids, propionate has been found to modulate the expression of proteins involved in cell cycle control, adipocyte function, and lipid metabolism (*54*). Propionate has also been shown to inhibit histone deacetylases and activate G protein–coupled receptor 43 and signal transducer and activator of transcription 3 (STAT3) to modulate intestinal epithelial cell migration both in vitro and in vivo (*55*).

In this study, we presented data indicating that two antibiotics that can suppress relative abundances of *Akkermansia*, azithromycin and tetracycline, may mediate protection against toxicities arising from systemic cytotoxic cancer therapy including total body RT. Fluoroquinolones have been best studied as prophylaxis and are recommended by guidelines (*5*) but are not active against most isolates of *A. muciniphila* (*56*). Recommending azithromycin as prophylaxis, however, can be problematic. In 2018, the U.S. Food and Drug Administration (FDA) released a warning regarding a potential increased risk of cancer relapse and death with azithromycin use after allogeneic HCT based on the ALLOZITHRO randomized clinical trial, a trial that was stopped early due to an imbalance in relapsed disease (*57*). Although subsequent retrospective studies have not reproduced this association (*58*), identifying antibiotics besides azithromycin that have activity against *Akkermansia* and other mucin-degrading bacteria could be a translational strategy to minimize risk for fever in neutropenic patients.

In summary, we found that the intestinal microbiome of patients who developed fever in the setting of neutropenia was enriched in mucin-degrading bacteria. Further experimentation in mice identified interrelated aspects of diet, metabolites, and intestinal mucus. These results suggest that development of novel approaches, including dietary, metabolite, pH, and antibacterial strategies, can potentially better prevent fevers in the setting of neutropenia after cancer therapy.

MATERIALS AND METHODS

Study design

This study aimed to investigate the role of the gut microbiome and diet-derived metabolites in developing neutropenic fever among cancer patients in the setting of radiation and chemotherapy. We first examined a link between the gut microbiome and fever in a cohort of 119 patients who had undergone HCT at the MD Anderson Cancer Center. To further understand the mechanism of the pathophysiology of neutropenic fever and to develop potential therapy, we used preclinical mouse models of irradiation, chemotherapy, and calorie restriction. Toward this, we conducted in vivo (SPF mice and germ-free mice) and in vitro experiments using different approaches. Informed consent was obtained with the MD Anderson Cancer Center Institutional Review Board approval (PA17-0035). The Institutional Animal Care and Use Committees (IACUCs) at the MD Anderson Cancer Center approved all the animal studies (IACUC 1705). More details can be found in the Supplementary Materials.

Human samples

Stool biospecimen collection from patients was approved by the University of Texas MD Anderson's Institutional Review Board, and signed informed consent was provided by all study participants. Samples were collected from patients undergoing stem cell transplantation and stored at 4°C for up to 48 hours before they were aliquoted for long-term storage at −80°C. Neutropenia was defined as a total white blood cell count less than 500 per microliter of blood. Neutropenic onset stool samples collected between day −2 and day +2 relative to the first day of neutropenia were eligible for inclusion in the study. Patients who received antibiotics other than standard bacterial prophylaxis with levofloxacin during the hospitalization before collection of neutropenic onset stool samples were excluded. Fever was defined as an oral temperature greater than 38.0°C within 4 days of neutropenic onset stool sample collection. For paired microbiome analyses, baseline stool samples were collected between 16 and 4 days (median of 5.5 days) before neutropenic onset samples.

Mice

Studies in animal models conformed to the *Guide for the Care and Use of Laboratory Animals* published by the U.S. National Institutes of Health and were approved by the IACUC. Six- to 8-week-old female C57BL/6 mice were obtained from the Jackson Laboratory. Six- to 8-week-old female C57BL/6 germ-free mice for murine studies were provided by the gnotobiotic facility of Baylor College of Medicine (Houston, TX).

Total body RT

Mice were exposed to a single myeloablative dose of total body RT (9-Gy RT) using a Shepherd Mark I, Model 30, 137Cs irradiator.

Murine temperature monitoring

Ocular temperatures were measured using an infrared FLIR E60 camera (FLIR) as previously described (*9*). Briefly, a 20-mm lens was attached to the front of the camera using a three-dimensional printed lens holder without any modifications to the camera for close-up imaging. Ocular temperatures were acquired with a 56-mm focal distance perpendicular to the eye being assessed. Data were analyzed by FLIR Tools+ software.

Patient avatar mice

Patient stool samples were suspended at a concentration of 50 mg of stool per milliliter of anaerobic phosphate-buffered saline (PBS), strained through a 100-μm cell strainer, and introduced to germ-free mice by gavage (200 μl) 14 days before RT.

A. muciniphila mono-associated mice

All animal procedures were conducted in compliance with Baylor College of Medicine IACUC-approved protocols. Germ-free C57BL/6J mice, 9 to 12 weeks of age, were housed in sterile flexible film isolators. Germ-free status was confirmed by fecal collection before starting the study. Some mice were transferred to a new isolator and treated with oral gavage of 10^8 colony-forming units of *A. muciniphila* (MDA-JAX AM001) in 0.2 ml of PBS. After 14 days, both groups of mice were euthanized via inhaled carbon dioxide.

Statistical analysis

Data were checked for normality and similar variances between groups, and Student's *t* tests and Pearson's correlation were used when appropriate. Mann-Whitney *U* tests and Spearman correlation were used to compare data between two groups when the data did not follow a normal distribution. Analyses were performed using R software version 3.6.0 and Prism version 7.0 (GraphPad Software). *P* values of <0.05 were considered statistically significant.

Supplementary Materials

This PDF file includes:
Materials and Methods
Figs. S1 to S8
Table S1
References (*12*, *18*, *59*–*81*)

Other Supplementary Material for this manuscript includes the following:
Data file S1
MDAR Reproducibility Checklist

View/request a protocol for this paper from *Bio-protocol*.

REFERENCES AND NOTES

1. N. M. Kuderer, D. C. Dale, J. Crawford, L. E. Cosler, G. H. Lyman, Mortality, morbidity, and cost associated with febrile neutropenia in adult cancer patients. *Cancer* **106**, 2258–2266 (2006).
2. E. Tai, G. P. Guy, A. Dunbar, L. C. Richardson, Cost of cancer-related neutropenia or fever hospitalizations, United States, 2012. *J. Oncol. Pract.* **13**, e552–e561 (2017).
3. R. A. Taplitz, E. B. Kennedy, E. J. Bow, J. Crews, C. Gleason, D. K. Hawley, A. A. Langston, L. J. Nastoupil, M. Rajotte, K. V. Rolston, L. Strasfeld, C. R. Flowers, Antimicrobial prophylaxis for adult patients with cancer-related immunosuppression: ASCO and IDSA clinical practice guideline update. *J. Clin. Oncol.* **36**, 3043–3054 (2018).
4. G. P. Bodey, The changing face of febrile neutropenia—From monotherapy to moulds to mucositis. Fever and neutropenia: The early years. *J. Antimicrob. Chemother.* **63**Suppl 1, i3-i13 (2009).
5. A. G. Freifeld, E. J. Bow, K. A. Sepkowitz, M. J. Boeckh, J. I. Ito, C. A. Mullen, I. I. Raad, K. V. Rolston, J. A. Young, J. R. Wingard; Infectious Diseases Society of America, Infectious diseases society of america, clinical practice guideline for the use of antimicrobial agents in neutropenic patients with cancer: 2010 update by the infectious diseases society of america. *Clin. Infect. Dis.* **52**, e56–e93 (2011).
6. F. B. Tamburini, T. M. Andermann, E. Tkachenko, F. Senchyna, N. Banaei, A. S. Bhatt, Precision identification of diverse bloodstream pathogens in the gut microbiome. *Nat. Med.* **24**, 1809–1814 (2018).
7. T. Rattanathammethee, P. Tuitemwong, P. Thiennimitr, P. Sarichai, S. Na Pombejra, P. Piriyakhuntorn, S. Hantrakool, C. Chai-Adisaksopha, E. Rattarittamrong, A. Tantiworawit, L. Norasetthada, Gut microbiota profiles of treatment-naive adult acute myeloid leukemia patients with neutropenic fever during intensive chemotherapy. *PLOS ONE* **15**, e0236460 (2020).
8. A. Rashidi, M. Ebadi, T. U. Rehman, H. Elhusseini, H. Halaweish, S. G. Holtan, S. Ramamoorthy, D. J. Weisdorf, A. Khoruts, C. Staley, Loss of microbiota-derived protective metabolites after neutropenic fever. *Sci. Rep.* **12**, 6244 (2022).
9. R. Masetti, F. D'Amico, D. Zama, D. Leardini, E. Muratore, M. Ussowicz, J. Fraczkiewicz, S. Cesaro, G. Caddeo, V. Pezzella, T. Belotti, F. Gottardi, P. Tartari, P. Brigidi, S. Turroni, A. Prete, Febrile neutropenia duration is associated with the severity of gut microbiota dysbiosis in pediatric allogeneic hematopoietic stem cell transplantation recipients. *Cancers (Basel)* **14**, 1932 (2022).
10. Y. Taur, J. B. Xavier, L. Lipuma, C. Ubeda, J. Goldberg, A. Gobourne, Y. J. Lee, K. A. Dubin, N. D. Socci, A. Viale, M. A. Perales, R. R. Jenq, M. van den Brink, E. G. Pamer, Intestinal domination and the risk of bacteremia in patients undergoing allogeneic hematopoietic stem cell transplantation. *Clin. Infect. Dis.* **55**, 905–914 (2012).
11. J. F. Sicard, G. Le Bihan, P. Vogeleer, M. Jacques, J. Harel, Interactions of intestinal bacteria with components of the intestinal mucus. *Front. Cell. Infect. Microbiol.* **7**, 387 (2017).

12. M. Kilcoyne, J. Q. Gerlach, M. P. Farrell, V. P. Bhavanandan, L. Joshi, Periodic acid-Schiff's reagent assay for carbohydrates in a microtiter plate format. *Anal. Biochem.* **416**, 18–26 (2011).
13. B. Vogel, H. Wagner, J. Gmoser, A. Worner, A. Loschberger, L. Peters, A. Frey, U. Hofmann, S. Frantz, Touch-free measurement of body temperature using close-up thermography of the ocular surface. *MethodsX* **3**, 407–416 (2016).
14. A. A. Romanovsky, M. C. Almeida, D. M. Aronoff, A. I. Ivanov, J. P. Konsman, A. A. Steiner, V. F. Turek, Fever and hypothermia in systemic inflammation: Recent discoveries and revisions. *Front. Biosci.* **10**, 2193–2216 (2005).
15. W. Tao, D. J. Deyo, D. L. Traber, W. E. Johnston, E. R. Sherwood, Hemodynamic and cardiac contractile function during sepsis caused by cecal ligation and puncture in mice. *Shock* **21**, 31–37 (2004).
16. I. Lagkouvardos, T. R. Lesker, T. C. A. Hitch, E. J. C. Galvez, N. Smit, K. Neuhaus, J. Wang, J. F. Baines, B. Abt, B. Stecher, J. Overmann, T. Strowig, T. Clavel, Sequence and cultivation study of Muribaculaceae reveals novel species, host preference, and functional potential of this yet undescribed family. *Microbiome* **7**, 28 (2019).
17. B. Gyurkocza, B. M. Sandmaier, Conditioning regimens for hematopoietic cell transplantation: One size does not fit all. *Blood* **124**, 344–353 (2014).
18. E. Ansaldo, L. C. Slayden, K. L. Ching, M. A. Koch, N. K. Wolf, D. R. Plichta, E. M. Brown, D. B. Graham, R. J. Xavier, J. J. Moon, G. M. Barton, *Akkermansia muciniphila* induces intestinal adaptive immune responses during homeostasis. *Science* **364**, 1179–1184 (2019).
19. M. E. Johansson, H. E. Jakobsson, J. Holmen-Larsson, A. Schutte, A. Ermund, A. M. Rodriguez-Pineiro, L. Arike, C. Wising, F. Svensson, F. Backhed, G. C. Hansson, Normalization of host intestinal mucus layers requires long-term microbial colonization. *Cell Host Microbe* **18**, 582–592.
20. J. M. Macy, L. G. Ljungdahl, G. Gottschalk, Pathway of succinate and propionate formation in *Bacteroides fragilis*. *J. Bacteriol.* **134**, 84–91 (1978).
21. M. D. Berkhout, C. M. Plugge, C. Belzer, How microbial glycosyl hydrolase activity in the gut mucosa initiates microbial cross-feeding. *Glycobiology* **32**, 182–200 (2022).
22. A. Benitez-Paez, E. M. Gomez Del Pulgar, Y. Sanz, The glycolytic versatility of bacteroides uniformis CECT 7771 and its genome response to oligo and polysaccharides. *Front. Cell. Infect. Microbiol.* **7**, 383 (2017).
23. H. Gamage, R. W. W. Chong, D. Bucio-Noble, L. Kautto, A. A. Hardikar, M. S. Ball, M. P. Molloy, N. H. Packer, I. T. Paulsen, Changes in dietary fiber intake in mice reveal associations between colonic mucin O-glycosylation and specific gut bacteria. *Gut Microbes* **12**, 1802209 (2020).
24. F. C. Pereira, K. Wasmund, I. Cobankovic, N. Jehmlich, C. W. Herbold, K. S. Lee, B. Sziranyi, C. Vesely, T. Decker, R. Stocker, B. Warth, M. von Bergen, M. Wagner, D. Berry, Rational design of a microbial consortium of mucosal sugar utilizers reduces *Clostridiodes difficile* colonization. *Nat. Commun.* **11**, 5104 (2020).
25. P. Ruas-Madiedo, M. Gueimonde, M. Fernandez-Garcia, C. G. de los Reyes-Gavilan, A. Margolles, Mucin degradation by *Bifidobacterium* strains isolated from the human intestinal microbiota. *Appl. Environ. Microbiol.* **74**, 1936–1940 (2008).
26. E. H. Crost, G. Le Gall, J. A. Laverde-Gomez, I. Mukhopadhya, H. J. Flint, N. Juge, Mechanistic insights into the cross-feeding of *Ruminococcus gnavus* and *Ruminococcus bromii* on host and dietary carbohydrates. *Front. Microbiol.* **9**, 2558 (2018).
27. E. H. Crost, L. E. Tailford, G. Le Gall, M. Fons, B. Henrissat, N. Juge, Utilisation of mucin glycans by the human gut symbiont *Ruminococcus gnavus* is strain-dependent. *PLOS ONE* **8**, e76341 (2013).
28. C. W. Png, S. K. Linden, K. S. Gilshenan, E. G. Zoetendal, C. S. McSweeney, L. I. Sly, M. A. McGuckin, T. H. Florin, Mucolytic bacteria with increased prevalence in IBD mucosa augment in vitro utilization of mucin by other bacteria. *Am. J. Gastroenterol.* **105**, 2420–2428 (2010).
29. M. Green, S. S. Cohen, Enzymatic conversion of L-fucose to L-fuculose. *J. Biol. Chem.* **219**, 557–568 (1956).
30. M. S. Desai, A. M. Seekatz, N. M. Koropatkin, N. Kamada, C. A. Hickey, M. Wolter, N. A. Pudlo, S. Kitamoto, N. Terrapon, A. Muller, V. B. Young, B. Henrissat, P. Wilmes, T. S. Stappenbeck, G. Nunez, E. C. Martens, A dietary fiber-deprived gut microbiota degrades the colonic mucus barrier and enhances pathogen susceptibility. *Cell* **167**, 1339–1353.e21 (2016).
31. T. R. Ziegler, M. Luo, C. F. Estivariz, D. A. Moore III, S. V. Sitaraman, L. Hao, N. Bazargan, J. M. Klapproth, J. Tian, J. R. Galloway, L. M. Leader, D. P. Jones, A. T. Gewirtz, Detectable serum flagellin and lipopolysaccharide and upregulated anti-flagellin and lipopolysaccharide immunoglobulins in human short bowel syndrome. *Am. J. Physiol. Regul. Integr. Comp. Physiol.* **294**, R402–R410 (2008).
32. L. Grimes, A. Doyle, A. L. Miller, R. B. Pyles, G. Olah, C. Szabo, S. Hoskins, T. Eaves-Pyles, Intraluminal flagellin differentially contributes to gut dysbiosis and systemic inflammation following burn injury. *PLOS ONE* **11**, e0166770 (2016).
33. J. Sun, X. Shen, Y. Li, Z. Guo, W. Zhu, L. Zuo, J. Zhao, L. Gu, J. Gong, J. Li, Therapeutic potential to modify the mucus barrier in inflammatory bowel disease. *Nutrients* **8**, 44 (2016).
34. Y. Shono, M. D. Docampo, J. U. Peled, S. M. Perobelli, E. Velardi, J. J. Tsai, A. E. Slingerland, O. M. Smith, L. F. Young, J. Gupta, S. R. Lieberman, H. V. Jay, K. F. Ahr, K. A. P. Rodriguez, K. Xu, M. Calarfiore, H. Poeck, S. Caballero, S. M. Devlin, F. Rapaport, J. A. Dudakov, A. M. Hanash, B. Gyurkocza, G. F. Murphy, C. Gomes, C. Liu, E. L. Moss, S. B. Falconer, A. S. Bhatt, Y. Taur, E. G. Pamer, M. R. van den Brink, R. R. Jenq, Increased GVHD-related mortality with broad-spectrum antibiotic use after allogeneic hematopoietic stem cell transplantation in human patients and mice. *Sci. Transl. Med.* **8**, 339ra371 (2016).
35. C. M. Dejea, P. Fathi, J. M. Craig, A. Boleij, R. Taddese, A. L. Geis, X. Wu, C. E. DeStefano Shields, E. M. Hechenbleikner, D. L. Huso, R. A. Anders, F. M. Giardiello, E. C. Wick, H. Wang, S. Wu, D. M. Pardoll, F. Housseau, C. L. Sears, Patients with familial adenomatous polyposis harbor colonic biofilms containing tumorigenic bacteria. *Science* **359**, 592–597 (2018).
36. M. Derrien, E. E. Vaughan, C. M. Plugge, W. M. de Vos, *Akkermansia muciniphila* gen. nov., sp. nov., a human intestinal mucin-degrading bacterium. *Int. J. Syst. Evol. Microbiol.* **54**, 1469–1476 (2004).
37. S. S. Seregin, N. Golovchenko, B. Schaf, J. Chen, N. A. Pudlo, J. Mitchell, N. T. Baxter, L. Zhao, P. D. Schloss, E. C. Martens, K. A. Eaton, G. Y. Chen, NLRP6 protects $Il10^{-/-}$ mice from colitis by limiting colonization of *Akkermansia muciniphila*. *Cell Rep.* **19**, 733–745 (2017).
38. S. M. Bloom, V. N. Bijanki, G. M. Nava, L. Sun, N. P. Malvin, D. L. Donermeyer, W. M. Dunne Jr., P. M. Allen, T. S. Stappenbeck, Commensal bacteroides species induce colitis in host-genotype-specific fashion in a mouse model of inflammatory bowel disease. *Cell Host Microbe* **9**, 390–403 (2011).
39. N. A. Pudlo, K. Urs, S. S. Kumar, J. B. German, D. A. Mills, E. C. Martens, Symbiotic human gut bacteria with variable metabolic priorities for host mucosal glycans. *MBio* **6**, e01282-01215 (2015).
40. A. Bell, J. Brunt, E. Crost, L. Vaux, R. Nepravishta, C. D. Owen, D. Latousakis, A. Xiao, W. Li, X. Chen, M. A. Walsh, J. Claesen, J. Angulo, G. H. Thomas, N. Juge, Elucidation of a sialic acid metabolism pathway in mucus-foraging *Ruminococcus gnavus* unravels mechanisms of bacterial adaptation to the gut. *Nat. Microbiol.* **4**, 2393–2404 (2019).
41. A. B. Hall, M. Yassour, J. Sauk, A. Garner, X. Jiang, T. Arthur, G. K. Lagoudas, T. Vatanen, N. Fornelos, R. Wilson, M. Bertha, M. Cohen, J. Garber, H. Khalili, D. Gevers, A. N. Ananthakrishnan, S. Kugathasan, E. S. Lander, P. Blainey, H. Vlamakis, R. J. Xavier, C. Huttenhower, A novel *Ruminococcus gnavus* clade enriched in inflammatory bowel disease patients. *Genome Med.* **9**, 103 (2017).
42. C. Depommier, A. Everard, C. Druart, H. Plovier, M. Van Hul, S. Vieira-Silva, G. Falony, J. Raes, D. Maiter, N. M. Delzenne, M. de Barsy, A. Loumaye, M. P. Hermans, J. P. Thissen, W. M. de Vos, P. D. Cani, Supplementation with *Akkermansia muciniphila* in overweight and obese human volunteers: A proof-of-concept exploratory study. *Nat. Med.* **25**, 1096–1103 (2019).
43. B. Routy, E. Le Chatelier, L. Derosa, C. P. M. Duong, M. T. Alou, R. Daillere, A. Fluckiger, M. Messaoudene, C. Rauber, M. P. Roberti, M. Fidelle, C. Flament, V. Poirier-Colame, P. Opolon, C. Klein, K. Iribarren, L. Mondragon, N. Jacquelot, B. Qu, G. Ferrere, C. Clemenson, L. Mezquita, J. R. Masip, C. Naltet, S. Brosseau, C. Kaderbhai, C. Richard, H. Rizvi, F. Levenez, N. Galleron, B. Quinquis, N. Pons, B. Ryffel, V. Minard-Colin, P. Gonin, J. C. Soria, E. Deutsch, Y. Loriot, F. Ghiringhelli, G. Zalcman, F. Goldwasser, B. Escudier, M. D. Hellmann, A. Eggermont, D. Raoult, L. Albiges, G. Kroemer, L. Zitvogel, Gut microbiome influences efficacy of PD-1-based immunotherapy against epithelial tumors. *Science* **359**, 91–97 (2018).
44. B. Becken, L. Davey, D. R. Middleton, K. D. Mueller, A. Sharma, Z. C. Holmes, E. Dallow, B. Remick, G. M. Barton, L. A. David, J. R. McCann, S. C. Armstrong, P. Malkus, R. H. Valdivia, Genotypic and phenotypic diversity among human isolates of *Akkermansia muciniphila*. *MBio* **12**, e00478-21 (2021).
45. C. Ozkul, M. Yalinay, T. Karakan, Islamic fasting leads to an increased abundance of *Akkermansia muciniphila* and *Bacteroides* fragilis group: A preliminary study on intermittent fasting. *Turk. J. Gastroenterol.* **30**, 1030–1035 (2019).
46. A. Basolo, M. Hohenadel, Q. Y. Ang, P. Piaggi, S. Heinitz, M. Walter, P. Walter, S. Parrington, D. D. Trinidad, R. J. von Schwartzenberg, P. J. Turnbaugh, J. Krakoff, Effects of underfeeding and oral vancomycin on gut microbiome and nutrient absorption in humans. *Nat. Med.* **26**, 589–598 (2020).
47. S. Verhoog, P. E. Taneri, Z. M. Roa Diaz, P. Marques-Vidal, J. P. Troup, L. Bally, O. H. Franco, M. Glisic, T. Muka, Dietary factors and modulation of bacteria strains of *Akkermansia muciniphila* and *Faecalibacterium prausnitzii*: A systematic review. *Nutrients* **11**, 1565 (2019).
48. L. Li, Y. Su, F. Li, Y. Wang, Z. Ma, Z. Li, J. Su, The effects of daily fasting hours on shaping gut microbiota in mice. *BMC Microbiol.* **20**, 65 (2020).
49. E. A. Miyasaka, Y. Feng, V. Poroyko, N. R. Falkowski, J. Erb-Downward, M. G. Gillilland III, K. L. Mason, G. B. Huffnagle, D. H. Teitelbaum, Total parenteral nutrition-associated lamina propria inflammation in mice is mediated by a MyD88-dependent mechanism. *J. Immunol.* **190**, 6607–6615 (2013).
50. S. Jeong, H. Y. Kim, A. R. Kim, C. H. Yun, S. H. Han, Propionate ameliorates staphylococcus aureus skin infection by attenuating bacterial growth. *Front. Microbiol.* **10**, 1363 (2019).
51. L. W. Chia, B. V. H. Hornung, S. Aalvink, P. J. Schaap, W. M. de Vos, J. Knol, C. Belzer, Deciphering the trophic interaction between *Akkermansia muciniphila* and the butyrogenic gut

commensal *Anaerostipes caccae* using a metatranscriptomic approach. *Antonie Van Leeuwenhoek* **111**, 859–873 (2018).
52. N. Ottman, M. Davids, M. Suarez-Diez, S. Boeren, P. J. Schaap, V. A. P. Martins Dos Santos, H. Smidt, C. Belzer, W. M. de Vos, Genome-scale model and omics analysis of metabolic capacities of *Akkermansia muciniphila* reveal a preferential mucin-degrading lifestyle. *Appl. Environ. Microbiol.* **83**, e01014-17 (2017).
53. M. T. Sorbara, K. Dubin, E. R. Littmann, T. U. Moody, E. Fontana, R. Seok, I. M. Leiner, Y. Taur, J. U. Peled, M. R. M. van den Brink, Y. Litvak, A. J. Baumler, J. L. Chaubard, A. J. Pickard, J. R. Cross, E. G. Pamer, Inhibiting antibiotic-resistant enterobacteriaceae by microbiota-mediated intracellular acidification. *J. Exp. Med.* **216**, 84–98 (2019).
54. S. Lukovac, C. Belzer, L. Pellis, B. J. Keijser, W. M. de Vos, R. C. Montijn, G. Roeselers, Differential modulation by *Akkermansia muciniphila* and *Faecalibacterium prausnitzii* of host peripheral lipid metabolism and histone acetylation in mouse gut organoids. *MBio* **5**, e01438-14 (2014).
55. A. J. Bilotta, C. Ma, W. Yang, Y. Yu, Y. Yu, X. Zhao, Z. Zhou, S. Yao, S. M. Dann, Y. Cong, Propionate enhances cell speed and persistence to promote intestinal epithelial turnover and repair. *Cell. Mol. Gastroenterol. Hepatol.* **11**, 1023–1044 (2021).
56. L. Maier, C. V. Goemans, J. Wirbel, M. Kuhn, C. Eberl, M. Pruteanu, P. Muller, S. Garcia-Santamarina, E. Cacace, B. Zhang, C. Gekeler, T. Banerjee, E. E. Anderson, A. Milanese, U. Lober, S. K. Forslund, K. R. Patil, M. Zimmermann, B. Stecher, G. Zeller, P. Bork, A. Typas, Unravelling the collateral damage of antibiotics on gut bacteria. *Nature* **599**, 120–124 (2021).
57. G. S. Cheng, L. Bondeelle, T. Gooley, Q. He, K. Jamani, E. F. Krakow, M. E. D. Flowers, R. P. de Latour, D. Michonneau, G. Socie, J. W. Chien, S. Chevret, A. Bergeron, Azithromycin use and increased cancer risk among patients with bronchiolitis obliterans after hematopoietic cell transplantation. *Biol. Blood Marrow Transplant.* **26**, 392–400 (2020).
58. J. L. Kutzke, J. A. Merten, J. L. Taraba, K. C. Mara, M. V. Shah, S. K. Hashmi, M. M. Patnaik, M. R. Litzow, W. J. Hogan, H. B. Alkhateeb, Risk of relapse in patients receiving azithromycin after allogeneic HSCT. *Bone Marrow Transplant.* **56**, 960–962 (2021).
59. L. R. Thompson, J. G. Sanders, D. McDonald, A. Amir, J. Ladau, K. J. Locey, R. J. Prill, A. Tripathi, S. M. Gibbons, G. Ackermann, J. A. Navas-Molina, S. Janssen, E. Kopylova, Y. Vázquez-Baeza, A. González, J. T. Morton, S. Mirarab, Z. Zech Xu, L. Jiang, M. F. Haroon, J. Kanbar, Q. Zhu, S. Jin Song, T. Kosciolek, N. A. Bokulich, J. Lefler, C. J. Brislawn, G. Humphrey, S. M. Owens, J. Hampton-Marcell, D. Berg-Lyons, V. McKenzie, N. Fierer, J. A. Fuhrman, A. Clauset, R. L. Stevens, A. Shade, K. S. Pollard, K. D. Goodwin, J. K. Jansson, J. A. Gilbert, R. Knight; Earth Microbiome Project Consortium, A communal catalogue reveals Earth's multiscale microbial diversity. *Nature* **551**, 457–463 (2017).
60. E. Bolyen, J. R. Rideout, M. R. Dillon, N. A. Bokulich, C. C. Abnet, G. A. al-Ghalith, H. Alexander, E. J. Alm, M. Arumugam, F. Asnicar, Y. Bai, J. E. Bisanz, K. Bittinger, A. Brejnrod, C. J. Brislawn, C. T. Brown, B. J. Callahan, A. M. Caraballo-Rodríguez, J. Chase, E. K. Cope, R. da Silva, C. Diener, P. C. Dorrestein, G. M. Douglas, D. M. Durall, C. Duvallet, C. F. Edwardson, M. Ernst, M. Estaki, J. Fouquier, J. M. Gauglitz, S. M. Gibbons, D. L. Gibson, A. Gonzalez, K. Gorlick, J. Guo, B. Hillmann, S. Holmes, H. Holste, C. Huttenhower, G. A. Huttley, S. Janssen, A. K. Jarmusch, L. Jiang, B. D. Kaehler, K. B. Kang, C. R. Keefe, P. Keim, S. T. Kelley, D. Knights, I. Koester, T. Kosciolek, J. Kreps, M. G. I. Langille, J. Lee, R. Ley, Y. X. Liu, E. Loftfield, C. Lozupone, M. Maher, C. Marotz, B. D. Martin, D. McDonald, L. J. McIver, A. V. Melnik, J. L. Metcalf, S. C. Morgan, J. T. Morton, A. T. Naimey, J. A. Navas-Molina, L. F. Nothias, S. B. Orchanian, T. Pearson, S. L. Peoples, D. Petras, M. L. Preuss, E. Pruesse, L. B. Rasmussen, A. Rivers, M. S. Robeson II, P. Rosenthal, N. Segata, M. Shaffer, A. Shiffer, R. Sinha, S. J. Song, J. R. Spear, A. D. Swafford, L. R. Thompson, P. J. Torres, P. Trinh, A. Tripathi, P. J. Turnbaugh, S. Ul-Hasan, J. J. J. van der Hooft, F. Vargas, Y. Vázquez-Baeza, E. Vogtmann, M. von Hippel, W. Walters, Y. Wan, M. Wang, J. Warren, K. C. Weber, C. H. D. Williamson, A. D. Willis, Z. Z. Xu, J. R. Zaneveld, Y. Zhang, Q. Zhu, R. Knight, J. G. Caporaso, Reproducible, interactive, scalable and extensible microbiome data science using QIIME 2. *Nat. Biotechnol.* **37**, 852–857 (2019).
61. T. Rognes, T. Flouri, B. Nichols, C. Quince, F. Mahe, VSEARCH: A versatile open source tool for metagenomics. *PeerJ* **4**, e2584 (2016).
62. R. C. Edgar, UNOISE2: Improved error-correction for Illumina 16S and ITS amplicon sequencing. bioRxiv 10.1101/081257 [Preprint]. 15 October 2016. ttps://doi.org/10.1101/081257.
63. P. D. Schloss, S. L. Westcott, T. Ryabin, J. R. Hall, M. Hartmann, E. B. Hollister, R. A. Lesniewski, B. B. Oakley, D. H. Parks, C. J. Robinson, J. W. Sahl, B. Stres, G. G. Thallinger, D. J. van Horn, C. F. Weber, Introducing mothur: Open-source, platform-independent, community-supported software for describing and comparing microbial communities. *Appl. Environ. Microbiol.* **75**, 7537–7541 (2009).
64. C. Quast, E. Pruesse, P. Yilmaz, J. Gerken, T. Schweer, P. Yarza, J. Peplies, F. O. Glöckner, The SILVA ribosomal RNA gene database project: Improved data processing and web-based tools. *Nucleic Acids Res.* **41**, D590–D596 (2013).
65. C. Lozupone, M. E. Lladser, D. Knights, J. Stombaugh, R. Knight, UniFrac: An effective distance metric for microbial community comparison. *ISME J.* **5**, 169–172 (2011).
66. M. E. Johansson, G. C. Hansson, Preservation of mucus in histological sections, immunostaining of mucins in fixed tissue, and localization of bacteria with FISH. *Methods Mol. Biol.* **842**, 229–235 (2012).
67. R. Li, H. Wang, Q. Shi, N. Wang, Z. Zhang, C. Xiong, J. Liu, Y. Chen, L. Jiang, Q. Jiang, Effects of oral florfenicol and azithromycin on gut microbiota and adipogenesis in mice. *PLOS ONE* **12**, e0181690 (2017).
68. A. M. Schubert, H. Sinani, P. D. Schloss, Antibiotic-induced alterations of the murine gut microbiota and subsequent effects on colonization resistance against clostridium difficile. *MBio* **6**, e00974 (2015).
69. S. Moosmang, M. Pitscheider, S. Sturm, C. Seger, H. Tilg, M. Halabalaki, H. Stuppner, Metabolomic analysis-addressing NMR and LC-MS related problems in human feces sample preparation. *Clin. Chim. Acta* **489**, 169–176 (2019).
70. Y. Sun, M. Bandi, T. Lofton, M. Smith, C. A. Bristow, A. Carugo, N. Rogers, P. Leonard, Q. Chang, R. Mullinax, J. Han, X. Shi, S. Seth, B. A. Meyers, M. Miller, L. Miao, X. Ma, N. Feng, V. Giuliani, M. G. Do, B. Czako, W. S. Palmer, F. Mseeh, J. M. Asara, Y. Jiang, P. Morlacchi, S. Zhao, M. Peoples, T. N. Tieu, M. O. Warmoes, P. L. Lorenzi, F. L. Muller, R. A. De Pinho, G. F. Draetta, C. Toniatti, P. Jones, T. P. Heffernan, J. R. Marszalek, Functional genomics reveals synthetic lethality between phosphogluconate dehydrogenase and oxidative phosphorylation. *Cell Rep.* **26**, 469–482.e5 (2019).
71. P. M. Smith, M. R. Howitt, N. Panikov, M. Michaud, C. A. Gallini, M. Bohlooly-Y, J. N. Glickman, W. S. Garrett, The microbial metabolites, short-chain fatty acids, regulate colonic Treg cell homeostasis. *Science* **341**, 569–573 (2013).
72. A. Bankevich, S. Nurk, D. Antipov, A. A. Gurevich, M. Dvorkin, A. S. Kulikov, V. M. Lesin, S. I. Nikolenko, S. Pham, A. D. Prjibelski, A. V. Pyshkin, A. V. Sirotkin, N. Vyahhi, G. Tesler, M. A. Alekseyev, P. A. Pevzner, SPAdes: A new genome assembly algorithm and its applications to single-cell sequencing. *J. Comput. Biol.* **19**, 455–477 (2012).
73. E. L. Sonnhammer, R. Durbin, A dot-matrix program with dynamic threshold control suited for genomic DNA and protein sequence analysis. *Gene* **167**, GC1–GC10 (1995).
74. T. Seemann, Prokka: Rapid prokaryotic genome annotation. *Bioinformatics* **30**, 2068–2069 (2014).
75. V. Lombard, H. Golaconda Ramulu, E. Drula, P. M. Coutinho, B. Henrissat, The carbohydrate-active enzymes database (CAZy) in 2013. *Nucleic Acids Res.* **42**, D490–D495 (2014).
76. H. Zhang, T. Yohe, L. Huang, S. Entwistle, P. Wu, Z. Yang, P. K. Busk, Y. Xu, Y. Yin, dbCAN2: A meta server for automated carbohydrate-active enzyme annotation. *Nucleic Acids Res.* **46**, W95–W101 (2018).
77. B. Buchfink, C. Xie, D. H. Huson, Fast and sensitive protein alignment using DIAMOND. *Nat. Methods* **12**, 59–60 (2015).
78. J. G. Caporaso, J. Kuczynski, J. Stombaugh, K. Bittinger, F. D. Bushman, E. K. Costello, N. Fierer, A. G. Peña, J. K. Goodrich, J. I. Gordon, G. A. Huttley, S. T. Kelley, D. Knights, J. E. Koenig, R. E. Ley, C. A. Lozupone, D. McDonald, B. D. Muegge, M. Pirrung, J. Reeder, J. R. Sevinsky, P. J. Turnbaugh, W. A. Walters, J. Widmann, T. Yatsunenko, J. Zaneveld, R. Knight, QIIME allows analysis of high-throughput community sequencing data. *Nat. Methods* **7**, 335–336 (2010).
79. H. Li, R. Durbin, Fast and accurate short read alignment with Burrows-Wheeler transform. *Bioinformatics* **25**, 1754–1760 (2009).
80. T. Tatusova, M. DiCuccio, A. Badretdin, V. Chetvernin, E. P. Nawrocki, L. Zaslavsky, A. Lomsadze, K. D. Pruitt, M. Borodovsky, J. Ostell, NCBI prokaryotic genome annotation pipeline. *Nucleic Acids Res.* **44**, 6614–6624 (2016).
81. M. I. Love, W. Huber, S. Anders, Moderated estimation of fold change and dispersion for RNA-seq data with DESeq2. *Genome Biol.* **15**, 550 (2014).

Acknowledgments: We thank the MD Anderson Cancer Center CCSG Microbiome core facility (NIH/NCI no. P30CA016672). We are thankful to the MD Anderson Cancer Center Metabolomics core facility supported by NIH (S10OD012304-01 and P30CA016672). The gnotobiotic studies were performed by the GEMS Gnotobiotic Core at Baylor College of Medicine, which is supported in part through the TMC DDC by NIH PHS grant P30KK056338. **Funding:** These studies were supported by R01HL124112 (NIH) and RR160089 (Cancer Prevention and Research Institute of Texas) to R.R.J.; S10OD012304 (NIH) and RP130397 (Cancer Prevention and Research Institute of Texas) to P.L.L.; K08HL143189 (NIH), P30CA008748 (NIH), and Parker Institute for Cancer Immunotherapy to J.U.P.; R01HL124112 (NIH) and P30CA016672 (NIH) to C.B.P.; and R01CA228358 (NIH), R01CA228308 (NIH), P30CA008748 (NIH), P01CA023766 (NIH), R01HL123340 (NHLBI), R01-HL147584 (NHLBI), and Tri-Institutional Stem Cell Initiative to M.R.M.v.d.B. M.R.M.v.d.B. received additional funding from the Lymphoma Foundation, the Susan and Peter Solomon Nutrition and Cancer Program, the Cycle for Survival, the Parker Institute for Cancer Immunotherapy, and the Paula and Rodger Riney Multiple Myeloma Research Initiative Fund. **Author contributions:** This project was conceptualized by Z.I.S., D.H.W., M.A.J., J.L.K., and R.R.J. Experiments were designed and conducted by Z.I.S., D.H.W., M.A.J., J.L.K., and R.R.J. Investigation was carried out by Z.I.S., D.H.W., C.-C.C., W.-B.T., D.P., S.S.A., T.H., M.R.O.T., R.K.E.-H., C.A.S., E.H., A.C.F.O., T.M., T.M.H., B.E.H., A.N.B., Y.J., M.R., R.P., I.F., L.M., V.C., P.L.L., M.O.W., L.T., A.G.S., S.F., M.C., K.M., T.G., V.B.J., C.B.P., K.-A.D., L.Z., Y. Shi, Y.W., J.R.G.-P., P.C.O.,

C.R.D.-M., Y. Shono, M.B.d.S., J.U.P., M.R.M.v.d.B., N.A., J.A.W., P.R., R.H.V., L.D., G.R., S. A. Srour, R.S.M., A.M.A., E.J.S., R.E.C., S. A. Shelburne, J.J.M., M.A.J., J.L.K., and R.R.J. Figures were generated by C.-C.C., M.A.J., J.L.K., and R.R.J. Funding was acquired by E.H., P.L.L., J.U.P., C.B.P., M.R.M.v.d.B., and R.R.J. Project administration was completed by M.A.J., J.L.K., and R.R.J. M.A.J., J.L.K., and R.R.J. supervised the project. Writing, review, and editing were done by Z.I.S., D.H.W., C.-C.C., M.A.J., J.L.K., and R.R.J. **Competing interests:** R.R.J. is an inventor and M.A.J., J.L.K., and E.H. are coinventors on a U.S. provisional patent application (serial no. 63/273,05) submitted by the University of Texas MD Anderson Cancer Center that covers methods and compositions for treating cancer therapy–induced neutropenic fever or GVHD. R.R.J. is on the advisory board for MaaT Pharma, LISCure Biosciences, Seres Therapeutics, Kaleido Biosciences, and Prolacta Bioscience. R.R.J. has consulted for Da Volterra, Merck, Microbiome Dx, and Karius. R.R.J. is an inventor on a patent (PCT/US2015/062734) that was licensed to Seres Therapeutics. M.R.M.v.d.B. has received research support and stock options from Seres Therapeutics and stock options from Notch Therapeutics and Pluto Therapeutics; has received royalties from Wolters Kluwer; has consulted and received honorarium from or participated in advisory boards for Seres Therapeutics, Vor Biopharma, Rheos Medicines, Frazier Healthcare Partners, Nektar Therapeutics, Notch Therapeutics, Ceramedix, LyGenesis, Pluto Therapeutics, GlaxoSmithKline, Da Volterra, Thymofox, Garuda, Novartis (Spouse), Synthekine (Spouse), BeiGene (Spouse), and Kite (Spouse); has IP Licensing with Seres Therapeutics and Juno Therapeutics; and holds a fiduciary role on the Foundation Board of DKMS (a nonprofit organization). MSK Cancer Center has institutional financial interests relative to Seres Therapeutics. R.H.V. is the founder of Bloom Science (San Diego, CA); the company was not involved in the funding of this work nor stands to benefit from its results. J.U.P. reports research funding, intellectual property fees, and travel reimbursement from Seres Therapeutics; holds equity in Postbiotics Plus Research; serves on an advisory board of Postbiotics Plus Research; and receives consulting fees from Da Volterra, CSL Behring, and MaaT Pharma. P.C.O. reports grant or research support from Merck Sharp & Dohme Corp., Napo Pharmaceuticals, Deinove, Summit Grant, and Melinta and paid consultancy for Napo Pharmaceuticals and Ferring Pharmaceuticals Inc. and has filed intellectual property applications related to the microbiome (reference numbers 62/843,849, 62/977,908, and 15/756,845). J.A.W. is an inventor on a U.S. patent application (PCT/US17/53.717) submitted by the University of Texas MD Anderson Cancer Center, which covers methods to enhance immune checkpoint blockade responses by modulating the microbiome; reports compensation for speaker's bureau and honoraria from Imedex, DAVA Oncology, Omniprex, Illumina, Gilead, PeerView, Physicians' Education Resource, MedImmune, Exelixis, and Bristol Myers Squibb; serves as a consultant/advisory board member for Roche/Genentech, Novartis, AstraZeneca, GlaxoSmithKline, Bristol Myers Squibb, Micronoma, Merck, and Biothera Pharmaceuticals; receives research support from GlaxoSmithKline, Roche/Genentech, Bristol Myers Squibb, and Novartis; and discloses additional patents WO2020150429A1, US20200129569A1, WO2019191390A2, and WO2020106983A1. A.G.S. is or has been a paid consultant for Diversigen, AbbVie, and Merck. **Data and materials availability:** All data associated with this study are present in the paper or the Supplementary Materials. All sequencing datasets are available in the NCBI BioProject database under accession number PRJNA858101.

Submitted 28 January 2022
Resubmitted 20 May 2022
Accepted 20 October 2022
Published 16 November 2022
10.1126/scitranslmed.abo3445

Science Translational Medicine

Diet-derived metabolites and mucus link the gut microbiome to fever after cytotoxic cancer treatment

Zaker I. Schwabkey, Diana H. Wiesnoski, Chia-Chi Chang, Wen-Bin Tsai, Dung Pham, Saira S. Ahmed, Tomo Hayase, Miriam R. Ortega Turrubiates, Rawan K. El-Himri, Christopher A. Sanchez, Eiko Hayase, Annette C. Frenk Oquendo, Takahiko Miyama, Taylor M. Halsey, Brooke E. Heckel, Alexandria N. Brown, Yimei Jin, Mathilde Raybaud, Rishika Prasad, Ivonne Flores, Lauren McDaniel, Valerie Chapa, Philip L. Lorenzi, Marc O. Warmoes, Lin Tan, Alton G. Swennes, Stephanie Fowler, Margaret Conner, Kevin McHugh, Tyler Graf, Vanessa B. Jensen, Christine B. Peterson, Kim-Anh Do, Liangliang Zhang, Yushu Shi, Yinghong Wang, Jessica R. Galloway-Pena, Pablo C. Okhuysen, Carrie R. Daniel-MacDougall, Yusuke Shono, Marina Burgos da Silva, Jonathan U. Peled, Marcel R.M. van den Brink, Nadim Ajami, Jennifer A. Wargo, Pavan Reddy, Raphael H. Valdivia, Lauren Davey, Gabriela Rondon, Samer A. Srour, Rohtesh S. Mehta, Amin M. Alousi, Elizabeth J. Shpall, Richard E. Champlin, Samuel A. Shelburne, Jeffrey J. Molldrem, Mohamed A. Jamal, Jennifer L. Karmouch, and Robert R. Jenq

Sci. Transl. Med. **14** (671), eabo3445. DOI: 10.1126/scitranslmed.abo3445

Fever and the gut

Chemotherapy lowers blood neutrophils and results in fever in some patients. Schwabkey *et al*. found that the gut microbiome may promote the onset of such neutropenic fever. Transferring gut microbiota from patients with neutropenic fever to irradiated mice promoted the development of subsequent fever. An excess of mucin-degrading *Akkermansia* bacteria found in the transferred microbiomes of febrile patients, as well as in nontransplanted but irradiated or chemotherapy-treated mice that reduced their food intake, resulted in a compromised intestinal barrier in mice that could be circumvented by administration of propionate. This study thus ties alterations in the gut microbiome to neutropenic fever and may provide a potential therapeutic strategy.

Science Translational Medicine (ISSN 1946-6242) is published by the American Association for the Advancement of Science. 1200 New York Avenue NW, Washington, DC 20005. The title *Science Translational Medicine* is a registered trademark of AAAS.